ENTLN Status Update

Stan Heckman[1]*

[1]Earth Networks, Germantown, Maryland, U.S.A.

ABSTRACT: Earth Networks records lightning electric field waveforms at 700 sites, and from those waveforms calculates latitudes, longitudes, and heights. The height errors are bigger than the latitude and longitude errors. This problem cannot be fixed; the height errors will always be bigger than the latitude and longitude errors. The network is built for for national storm monitoring and weather warnings, so it is designed to see cloud flashes over an entire country, with waveform recording sites typically 100 to 300 kilometers apart. Any time of arrival network with sites more than 100 kilometers apart will have larger vertical errors than horizontal errors because vertical changes in source location cause smaller time of arrival differences than horizontal changes in source location. Despite large height errors of individual pulses, we hope that heights will still be useful for monitoring time evolution of entire storms because, in the usual way that many noisy measurements can be combined into fewer less noisy measurements, many uncertain pulse heights can be combined into a few more certain source height density profiles versus time.

INTRODUCTION

The Earth Networks Total Lightning Network (ENTLN) consists of 700 sites that record vertical electric field from 1 Hz to 12 MHz. Pulses in electric field are located by time of arrival, and grouped into flashes. The focus of the network has been on detecting cloud flashes over entire countries for severe weather warning or other thunderstorm monitoring applications.

Thunderstorms matter. Much severe weather that kills people or destroys property is associated with severe thunderstorms. Like other clouds, thunderstorms are studied with satellites and radar. Unlike other clouds, thunderstorms can also be studied with lightning. Lightning gives different information than satellites and radar; some things satellites and radar see better than lightning, other things (like high time resolution cell locations and cell severities) lightning sees more easily than satellites and radar. Lightning location systems can also be cheaper than satellites and radar because kiloamp pulses radiated by kilometer tall antennas are relatively inexpensive to detect.

Monitoring thunderstorms using lightning works surprisingly well. Using only lightning, no satellite or radar data and no human intervention, Earth Networks generates severe weather (hail, tornado, strong wind) warnings in the US. These can't warn of any severe weather that doesn't include lightning, so they have poorer probability of detection than warnings that use satellite and radar. On the other hand, they have comparable false alarm rates and better lead times than the operational national weather service warnings that use satellite, radar, and human forecasters. In countries with radar, these computer generated warnings could be combined with radar, satellite, and expert human forecaster inputs to improve false alarm rate and lead time. In countries without radar, lightning alone could be used to deliver completely automated warnings.

Using only lightning, no radar, satellite, or human input, Earth Networks generates predicted radar reflectivity, vertically integrated liquid, and precipitation maps somewhat similar to maps made combining rain gauges, satellites, and radar. See figure 1. Again, in countries with radar, these could be combined with rain gauges, satellite and radar to make a better estimate than could be made without lightning. Or in countries without radar, this could be combined with satellite data to make less accurate but completely automated rain maps.

*Corresponding author, email: sheckman@earthnetworks.com

We want to improve our warnings and precipitation maps. In past years, we have tried to do that by improving our cloud flash detection efficiency. But now over the US we see five out of six of the flashes the LIS satellite sees, so we may be reaching the limits of how much we can improve our warnings by increasing our flash detection efficiency. We could work on our pulse detection efficiency instead, locating more pulses per flash, but today that wouldn't improve our warnings and precipitation maps because today, those maps are made using only the lightning flash rate, not the pulse rate. There is a lot more information in each lightning flash than where and when it occurred, but it isn't obvious what other lightning properties will be most useful. There are many possible properties to choose from. Should we use number of pulses, or flash area, or flash duration, or pulse type or what? We should not pick a property like "ratio of risetime to fall time of the pulse" because we have no reason to suspect that property is in any way related to storm severity. We also should not pick that property because no one else measures it, which means no one else will study it. We could choose number of pulses, but it isn't clear that that is related to storm severity either, nor is it clear that different systems will measure the same number of pulses. Wanting to improve something other than our detection efficiency, We chose "height" as the first new property to work on, because it seems plausible that changes in the heights of positive and negative charge layers are related to storm evolution, and because other systems (VHF mappers) can measure height, so other scientists might also study it.

LOCATION UNCERTAINTY

One electric field pulse received at several sites is shown in figure 2. This is the first of 24 pulses we located in this intracloud flash.

If there were no uncertainty in the timing measurement, then timing measurements at 4 sites would exactly determine the four unknowns latitude, longitude, height and time (y,x,z,t) that define the source location. But there is uncertainty in the timing measurement, so four measurements instead determine a probability distribution of possible x,y,z, and t values. In practice this probability distribution has intolerably large uncertainties if only 4 sites are used. The more sites that are used (and the better the measurements from the different sites agree) the smaller the uncertainty becomes.

Given the observed pulse arrival times at these sites, the probability that the source of the pulses was at x,y,z,t is (assuming a uniform prior) the product of the probabilities of observing each of these arrival times given that the source was at x,y,z,t. Figure 3 shows the measured probability of observing different timing errors in this network. This is the observed timing error at sites not included in the solution, measured over one million of pulses in multiple storms. This slightly overestimates the timing error, as the true timing error would be the difference between the measured time of arrival and the time of arrival computed using the true location of the flash, while we used instead the difference between the measured time of arrival and the time of arrival computed using our best estimate (from other sites) of flash location. So the error in figure 3 is really the sum of the single site timing error and our location error. We will ignore the location error contribution and pretend that figure 3 is the true single site timing error.

For each possible source location x,y,z,t, we compute the distance to each observing site, and from that the expected time of arrival of the pulse. The difference between the expected and observed time, together with figure 3, determines the probability of the observation given that the source location is x,y,z,t. By Bayes theorem, the product of these probabilities is proportional to the probability that the source location is x,y,z,t given these observations.

This probability density summed over z and t to produce a horizontal (xy) probability density is shown in figure 4. 3 contours of constant probability density are drawn. The innermost encloses 50% of the total probability; there is a 50% chance that the true location lies inside this contour. This contour is about 300 meters across. The middle contour encloses 90% of the total probability; this contour is about 600 meters across. The outer, irregularly shaped contour encloses 99% of the total probability. This contour is about

1.5 kilometers across at its widest point.

The probability density summed over x and t (or y and t) to produce a vertical probability density is shown in figure 5. The contours enclosing 50probability are still roughly 300 meters wide, but they are now about one kilometer tall. The contours enclosing 90are one and a half and two and a half kilometers tall. The uncertainties are always taller than they are wide. We don't know height as well as we know latitude and longitude.

The reason for this is that with sites 150 kilometers apart, a one kilometer change in height causes a smaller change in time difference of arrival than a one kilometer horizontal change. Consider a lightning pulse originating at 10 kilometers height, 50 kilometers east of one measuring site and 100 kilometers west of another site. The distance from the pulse to the first site is $\sqrt{50^2 + 10^2}$ kilometers. The distance to the second site is $\sqrt{100^2 + 10^2}$ kilometers. The time difference of arrival at the two sites is $(\sqrt{100^2 + 10^2} - \sqrt{50^2 + 10^2})/c$, which is 165.1 microseconds. If the lightning had occurred one kilometer to the west, the distances would have been $\sqrt{49^2 + 10^2}$ and $\sqrt{101^2 + 10^2}$, and the time difference of arrival would have been 172 microseconds. Figure 3 shows that our timing errors are usualy less than 7 microseconds, so it is easy to tell the difference between a 165 microsecond time delay and a 172 microsecond time delay, so we can expect better than one kilometer horizontal location accuracy. If the lightning had occurred one kilometer lower, then the distances would have been $\sqrt{50^2 + 10^2}$ and $\sqrt{100^2 + 10^2}$, with a time difference of 165.4 microseconds. Figure 3 shows that we often make 0.3 microsecond timing errors, so it is not so easy to tell the difference between a 165.1 microsecond time delay and a 165.4 microsecond time delay, so we cannot expect one kilometer vertical location accuracy for this hypothetical pulse.

This problem can be solved by putting the sites 15 kilometers apart instead of 150 kilometers apart. Unfortunately, that requires 100 times as many sites to cover the same area, and Earth Networks can't afford that many sites. So for the forseeable future, Earth Networks' vertical locations errors are going to be much bigger than their horizontal location errors.

ONE FLASH

Earth Networks locates 24 electric field pulses from the flash shown in figures 5 and 6. We compute location probability densities for each and compare to VHF source locations from the DC Lightning Mapping Array, a New Mexico Tech VHF time of arrival system owned and operated by NASA. The medium frequency electric field pulse locations are shown as a colored probability density and 3 black constant probability density contours containing 50%, 90%, and 99% of the total probability. VHF source locations within 5 milliseconds of the medium frequency electric field pulse are shown in green, VHF source locations earlier or later than this are shown in purple. The waveforms and locations of each of the 24 pulses are shown in figures 6 to 76. Sometimes the ENTLN probability distributions and the near simultaneous VHF locations are close to each other, and sometimes the VHF is at one edge of the flash while the ENTLN location is in the interior of the flash.

These plots also include red contours that show where 50%, 90%, and 99% of the probability density would have been located if we had assumed gaussian timing errors instead of assuming the measured timing error distribution from figure 3. The red contours are always smaller, indicating that had we believed our timing errors are gaussian, then we would also have believed our location errors were smaller. Unfortunately, our timing errors really aren't gaussian, so our location errors really aren't as small as the red ellipses predict.

A plot versus time of the most likely height of each pulse together with an error bar containing half the total likelyhood (figure 77) shows that this flash starts at 10 kilometers, then extends upward into a layer around 11 kilometers, and downward into a layer around 7 kilometers. The Earth Networks pulse locations are at the same general height as the VHF pulse locations at each time (first in the lower part until 1.6 seconds, then the upper part until 1.7 seconds, then back to the lower part after that.) The VHF system

sees many more pulses than Earth Networks sees in the upper part of the flash above the 10 km starting location, but they see about the same number of pulses in the lower part of the flash below the 10 km starting location. The vertical uncertainties of the Earth Networks locations are always quite large. This large height uncertainty makes a sparse network (like Earth Networks) a poor choice for making three dimensional maps of individual lightning channels; a denser network (like most VHF networks) is better for this task.

ACKNOWLEDGMENTS: VHF comparisons would not have been possible without NASA's continuing support for the DC LMA.

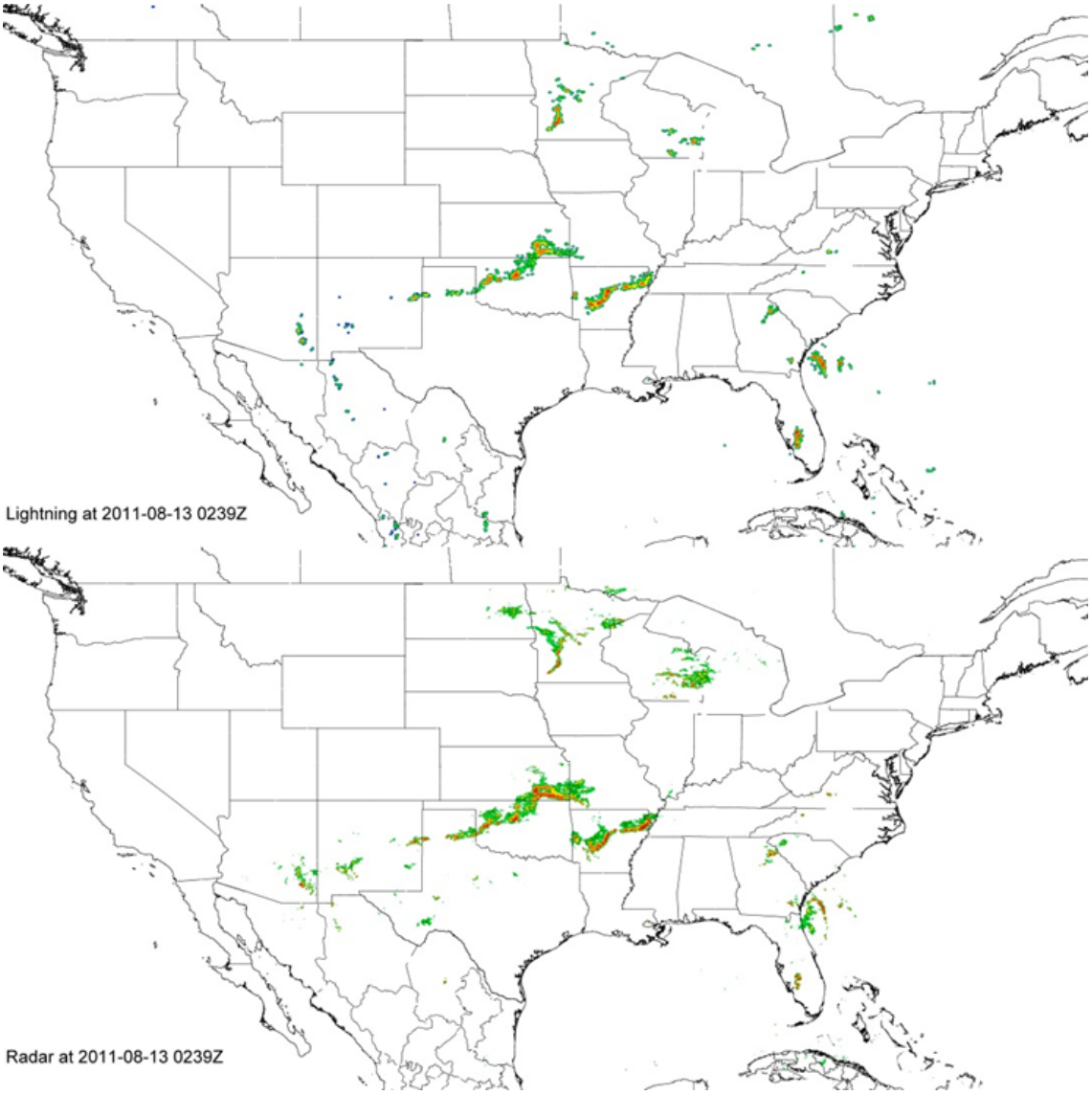

Figure 1: Precipitation estimate from lightning and precipitation estimate from radar

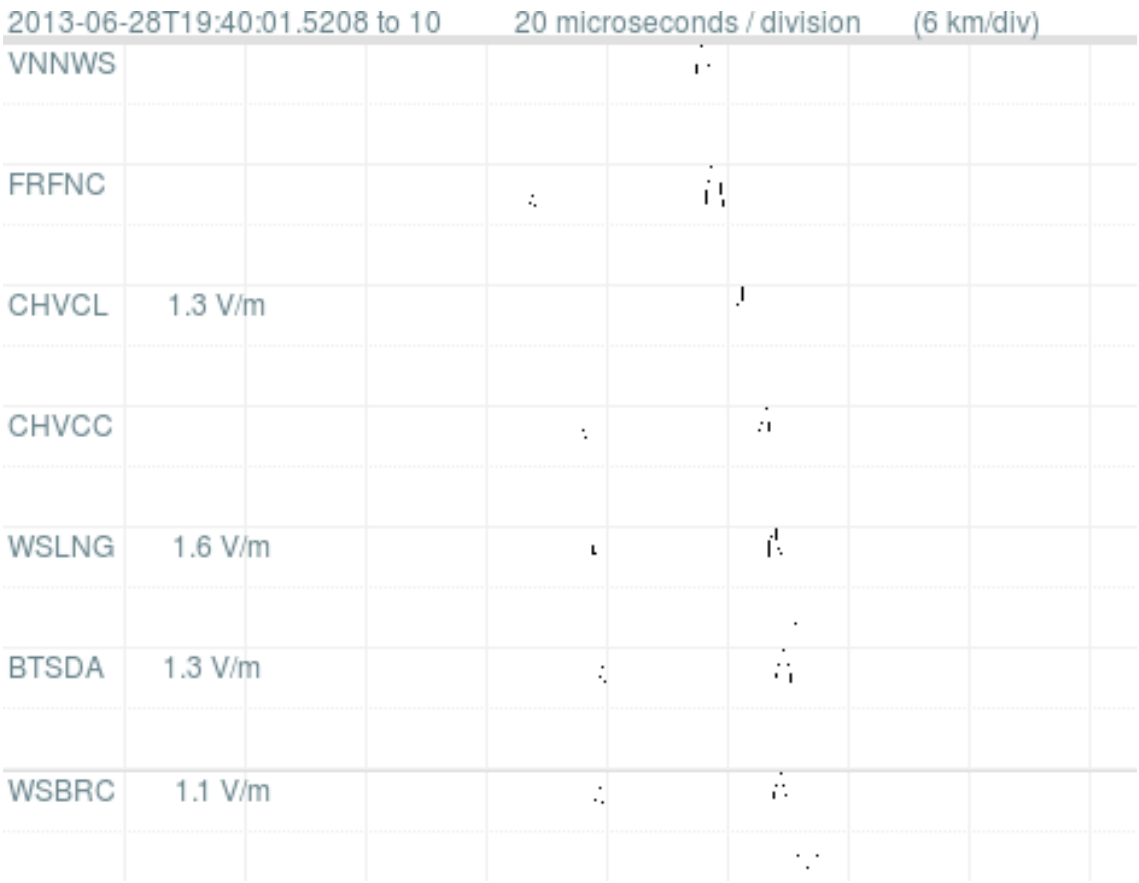

Figure 2: Electric field pulse at 7 sites. This is the first pulse we saw of this flash.

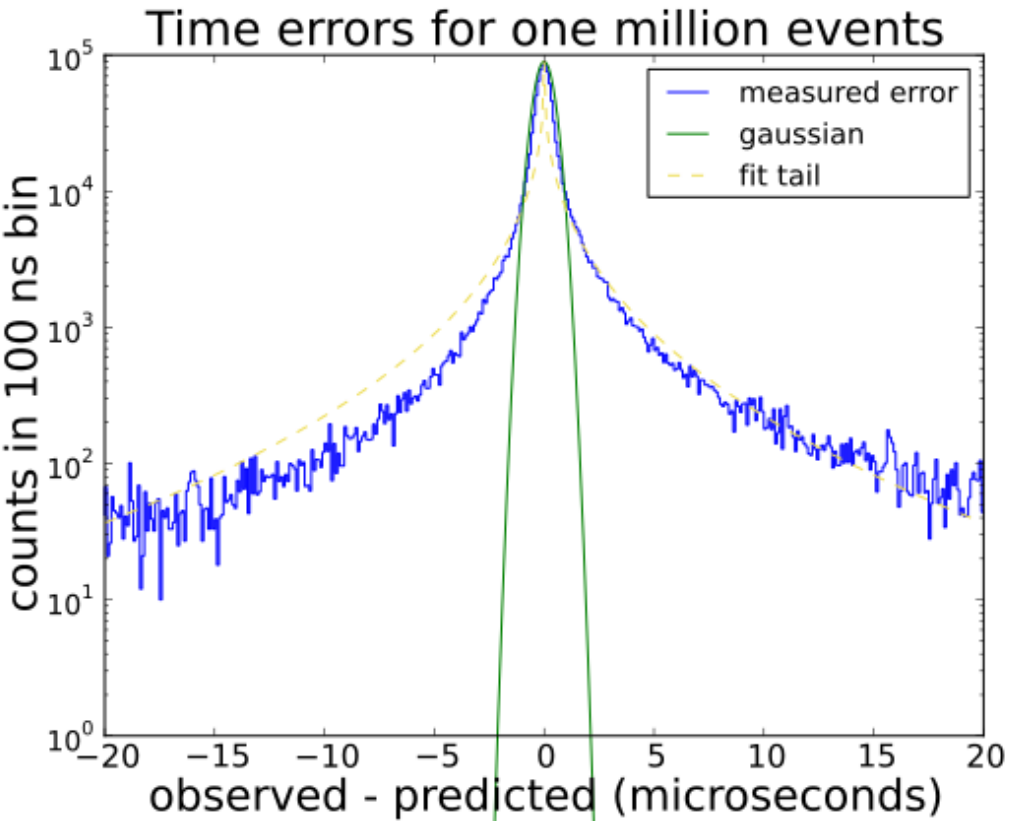

Figure 3: Observed timing errors of one million pulses in blue. Best fit Gaussian in green, best power law fit to the long tail in yellow. What is plotted is the difference between observed time of arrival and predicted time of arrival, so it is the sum of the single site timing error and the network location error.

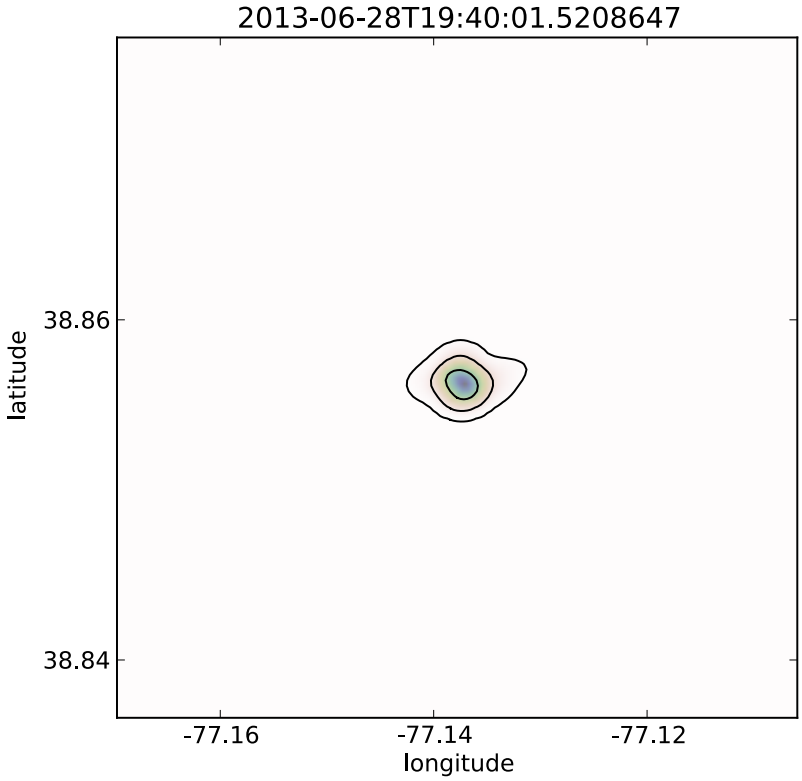

Figure 4: Probability density for the source location of the electric field pulses shown in figure 2. Three contours of constant probability density are drawn. The innermost contour contains 50% of the total probability, the middle contour contains 90%, and the outermost contour contains 99%.

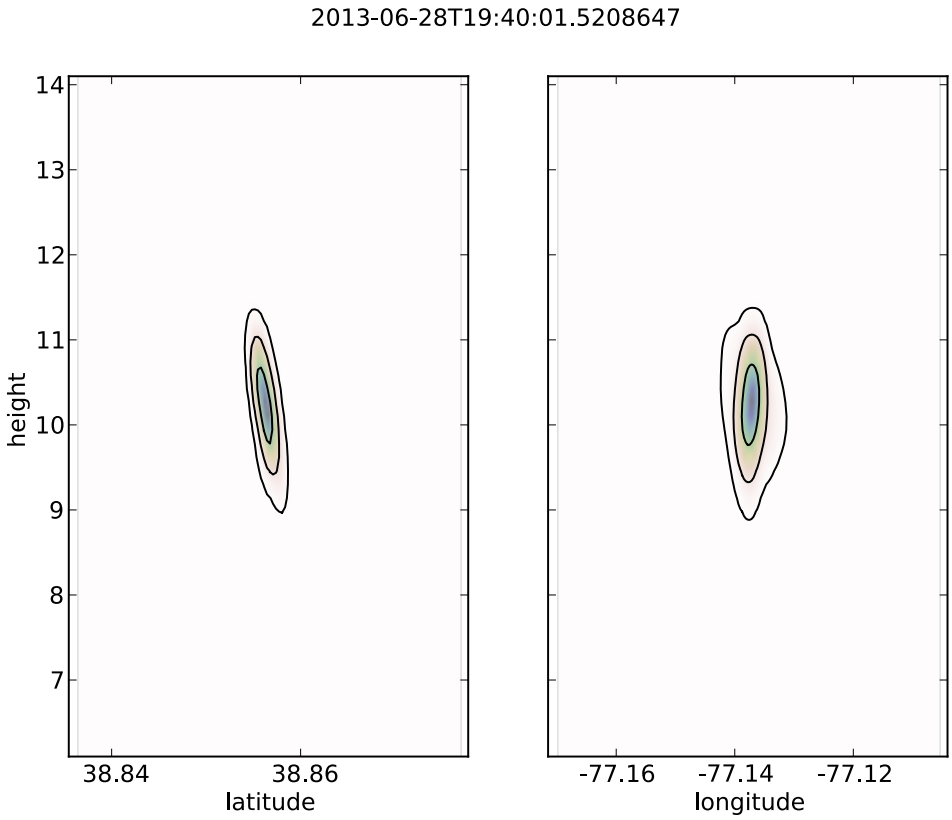

Figure 5: Probability density for the vertical source location of the electric field pulses shown in figure 2. Three contours of constant probability density are drawn. The innermost contour contains 50% of the total probability, the middle contour contains 90%, and the outermost contour contains 99%. The contours are taller than they are wide, which means the vertical location is more uncertain than the horizontal location.

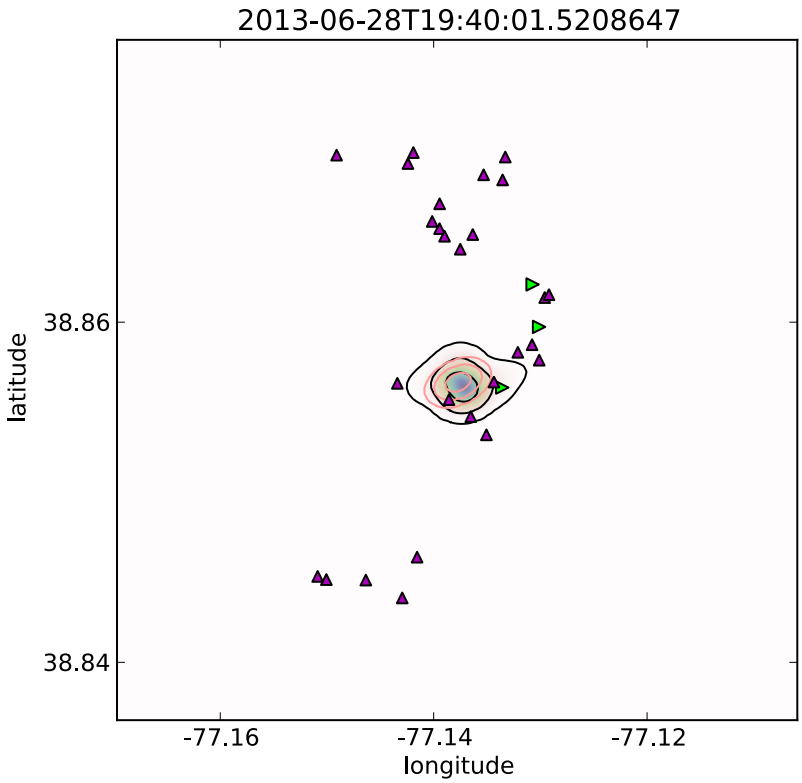

Figure 6: Probability density for horizontal source location of the first pulse of this flash, together with locations of VHF sources observed in the entire flash. Three levels of constant probability density are contoured in black, just as in figures 4. The innermost contour contains half the total probability. The middle contour contains 90% of the total probability, and the outer contour contains 99% of the total probability. Red contours show what we would have computed for 50%, 90%, and 99% contours if we had assumed that the timing errors of our system were Gaussian, instead of using the measured timing error from figure 3. The red contours are smaller, indicating that we would have thought that our locations were more precise if we thought our timing errors were Gaussian. Triangles show locations of VHF sources identified in this entire flash. Green triangles are VHF sources that occurred within 5 milliseconds of this pulse, purple triangles occurred more than 5 milliseconds after this pulse.

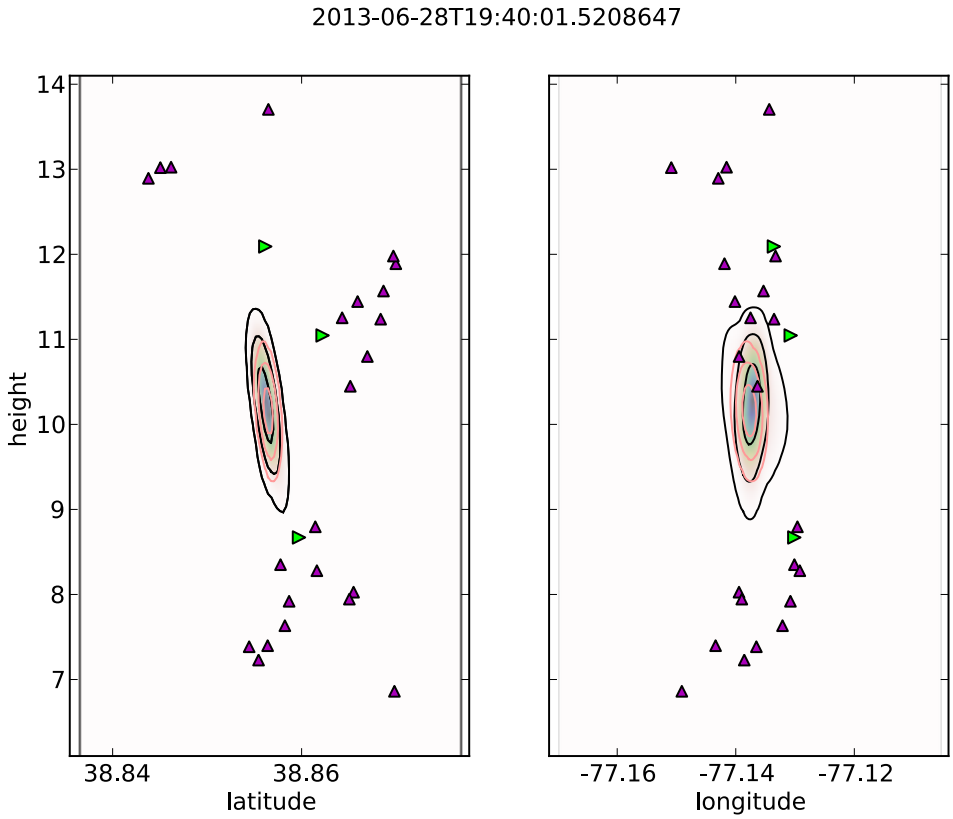

Figure 7: Probability density for vertical source location of the first pulse of this flash, together with locations of VHF sources observed in the entire flash. Three levels of constant probability density are contoured in black, containing 50%, 90%, and 99% of the total probability. Red contours show what we would have computed for 50%, 90%, and 99% contours if we had assumed that the timing errors of our system were Gaussian, instead of using the measured timing error from figure 3. Triangles show locations of VHF sources identified in this entire flash. Green triangles are VHF sources that occurred within 5 milliseconds of this pulse, purple triangles occurred more than 5 milliseconds after this pulse.

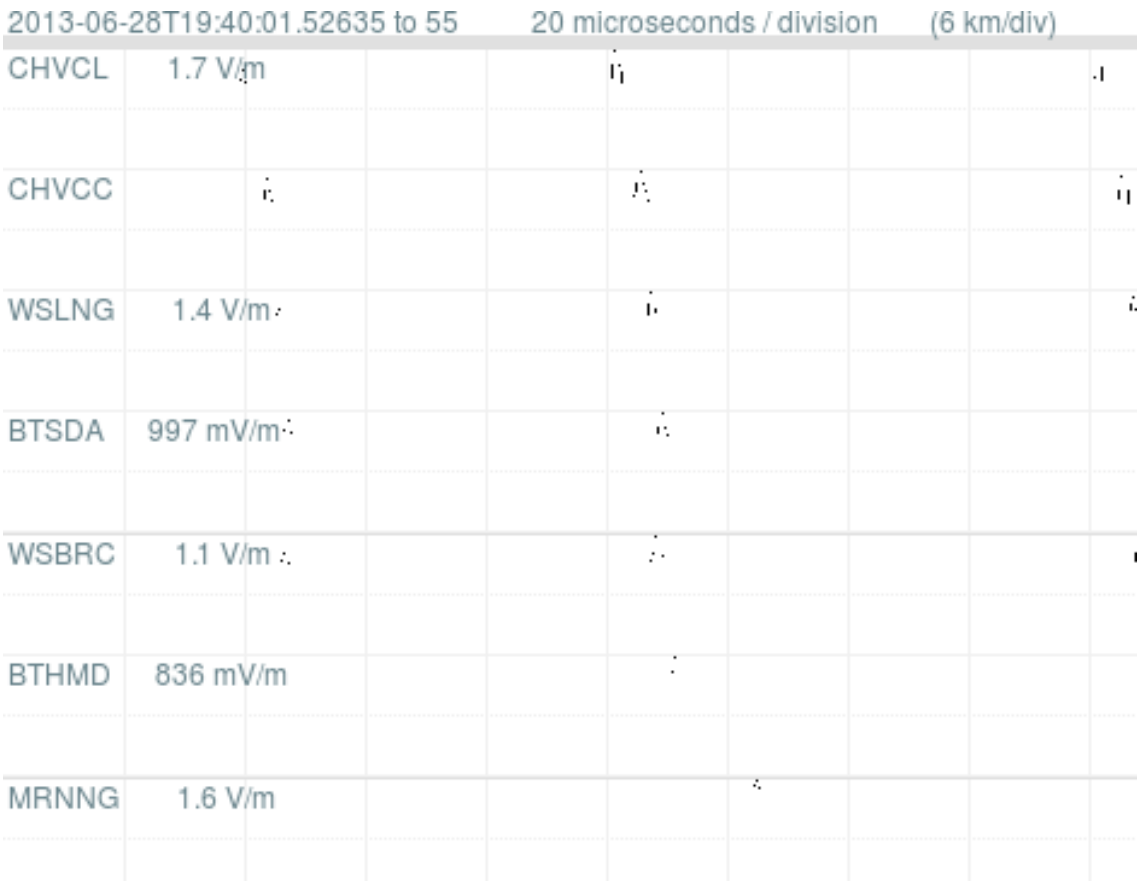

Figure 8: Electric field waveforms for second pulse of this flash.

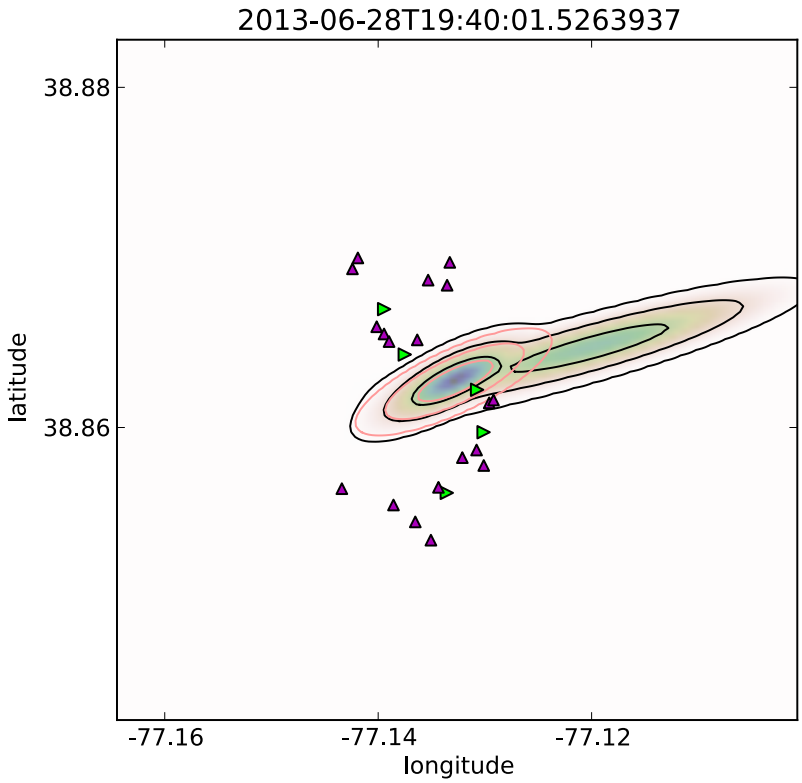

Figure 9: Probability density for source location of the second pulse of this flash. Three levels of constant probability density are contoured in black. The innermost contour, which is split into two disjoint sections, contains half the total probability. The middle contour contains 90% of the total probability, and the outer contour contains 99% of the total probability. Red contours show what we would have computed for 50%, 90%, and 99% contours if we had assumed that the timing errors of our system were Gaussian, instead of using the measured timing error from figure 3. Triangles show locations of VHF sources identified in this entire flash. Green triangles are VHF sources that occurred within 5 milliseconds of this pulse, purple triangles occurred more than 5 milliseconds after this pulse.

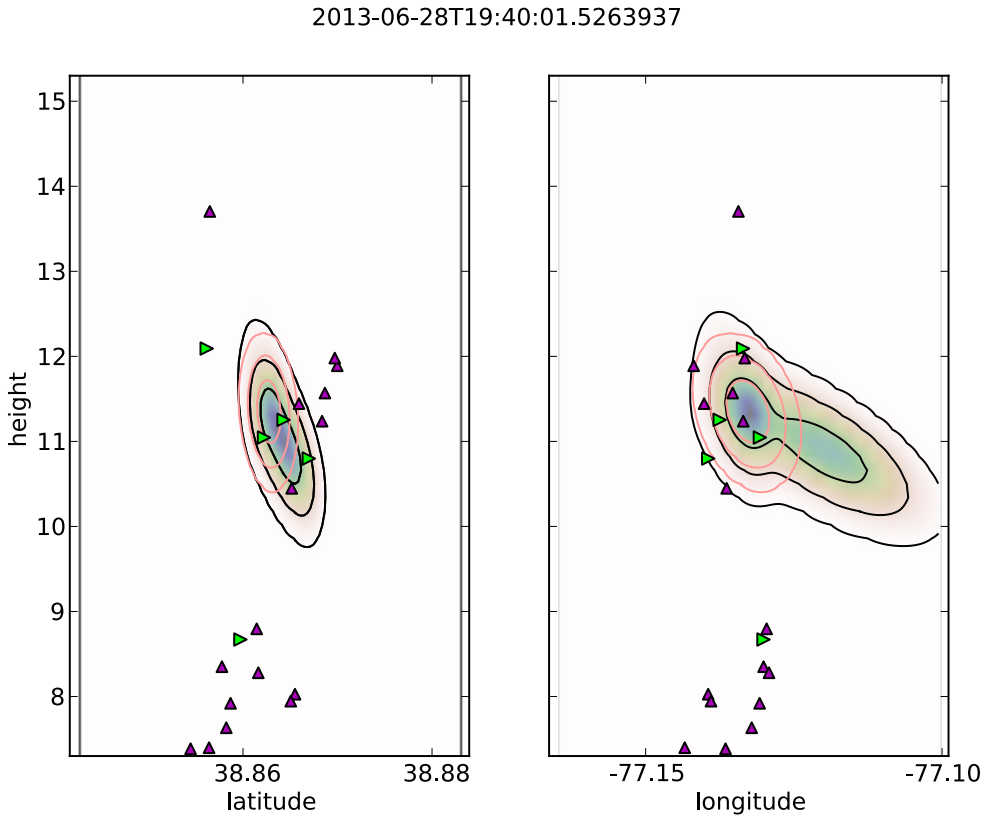

Figure 10: Probability density for vertical source location of the second pulse of this flash. Three levels of constant probability density containing 50%, 90%, and 99% of the total probability density are contoured in black. Red contours show what we would have computed for 50%, 90%, and 99% contours if we had assumed that the timing errors of our system were Gaussian, instead of using the measured timing error from figure 3. Triangles show locations of VHF sources identified in this entire flash. Green triangles are VHF sources that occurred within 5 milliseconds of this pulse, purple triangles occurred more than 5 milliseconds after this pulse. This pulse occurred higher than the first pulse, in what will become the upper layer of this flash.

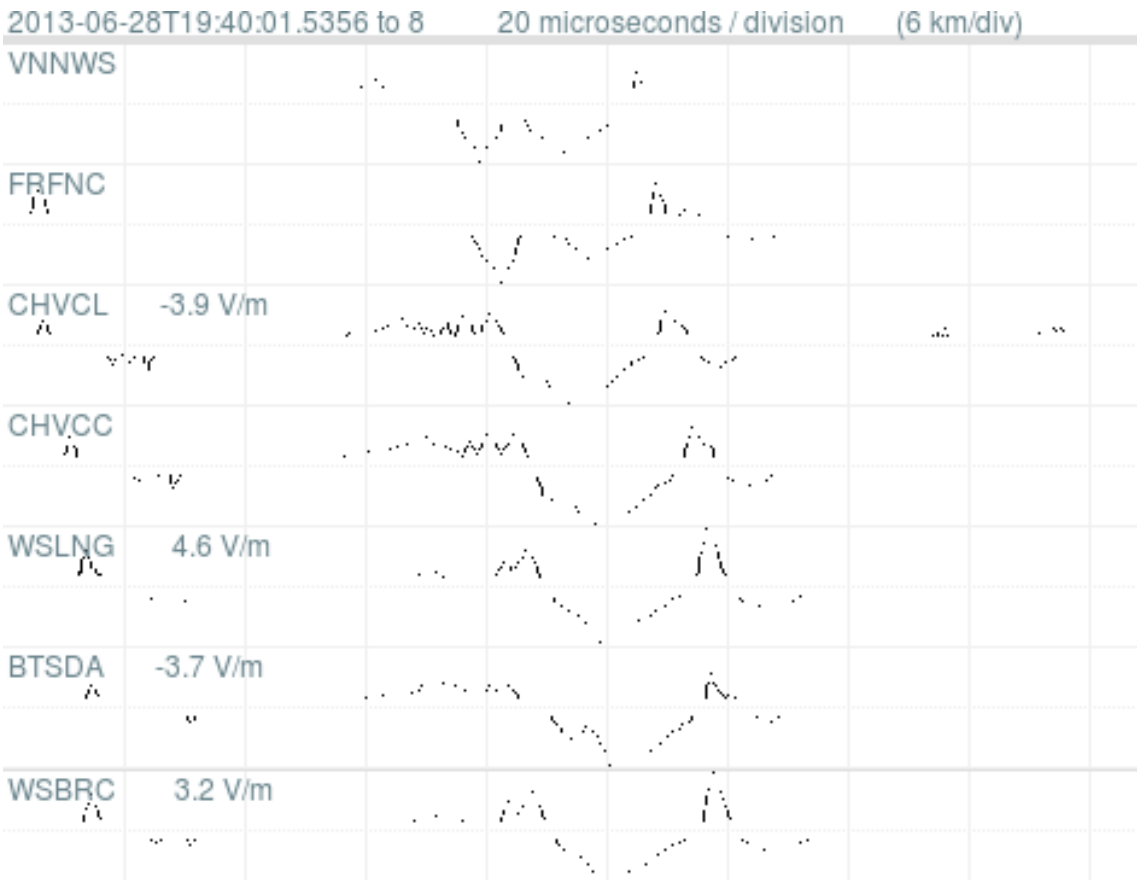

Figure 11: Electric field waveforms for third pulse of this flash. This pulse has a different shape than any of the other pulses in this flash, and no VHF sources were identified within 5 milliseconds of this pulse.

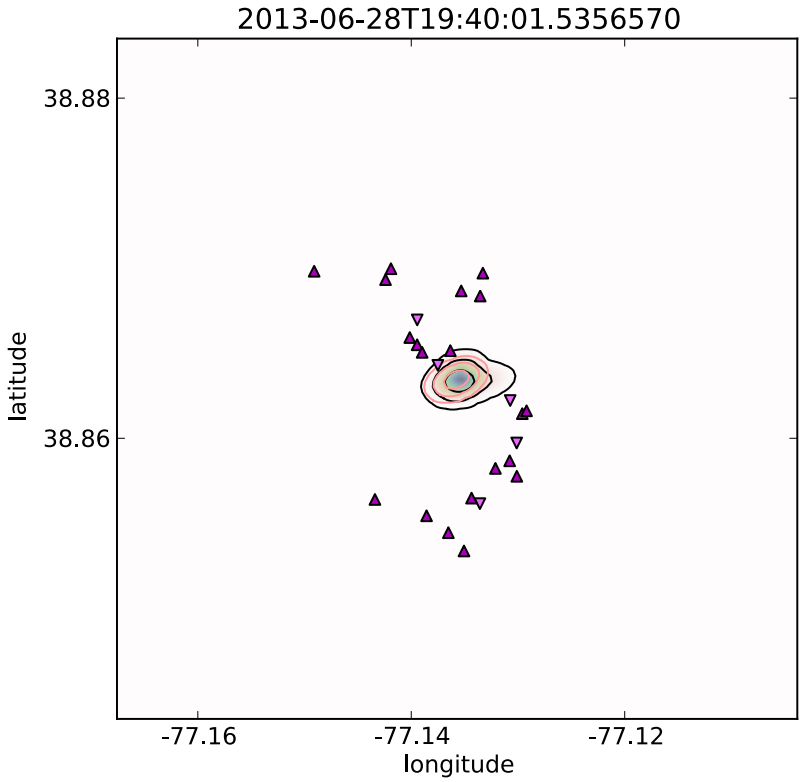

Figure 12: Probability density for source location of the third pulse of this flash. Constant probability density contours containing 50%, 90%, and 99% of the total probability are contoured in black. Red contours show what we would have computed for 50%, 90%, and 99% contours if we had assumed that the timing errors of our system were Gaussian, instead of using the measured timing error. Triangles show locations of VHF sources identified in this entire flash. There are no green triangles this time, because no VHF sources occurred within 5 milliseconds of this pulse.

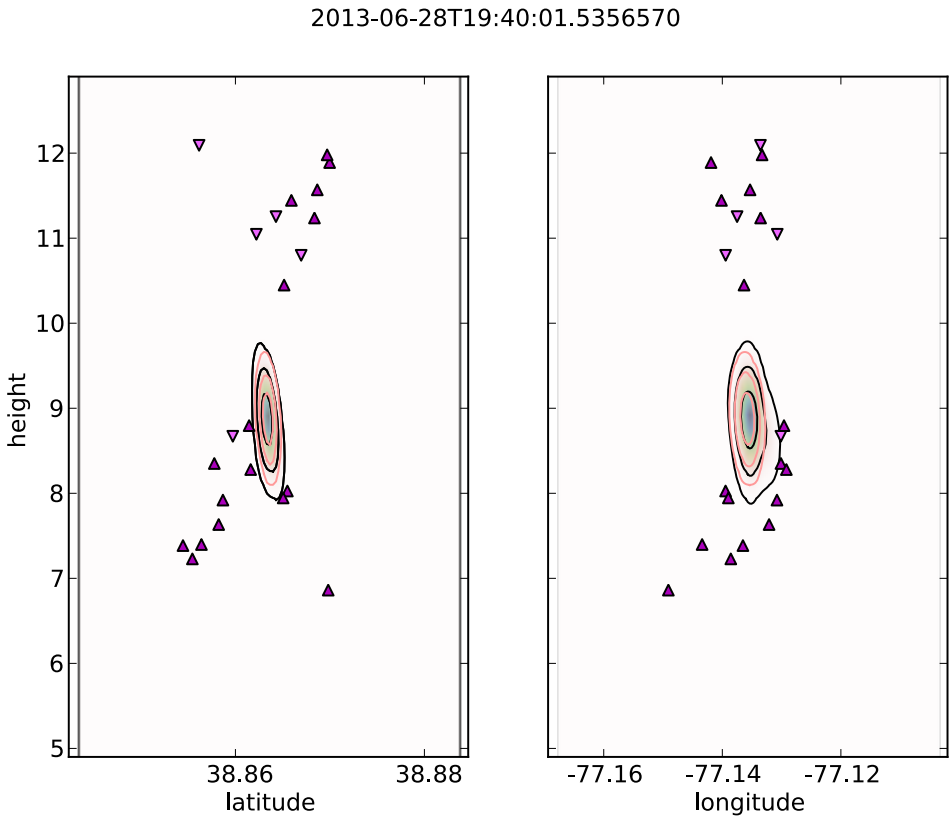

Figure 13: Probability density for vertical source location of the third pulse of this flash. Black constant probability density contours contain 50%, 90%, and 99% of the total probability as before. Red contours show what we would have computed for 50%, 90%, and 99% contours if we had assumed that the timing errors of our system were Gaussian. Triangles show locations of VHF sources identified in this flash. No VHF sources occurred within 5 milliseconds of this pulse.

Figure 14: Electric field waveforms for fourth pulse of this flash.

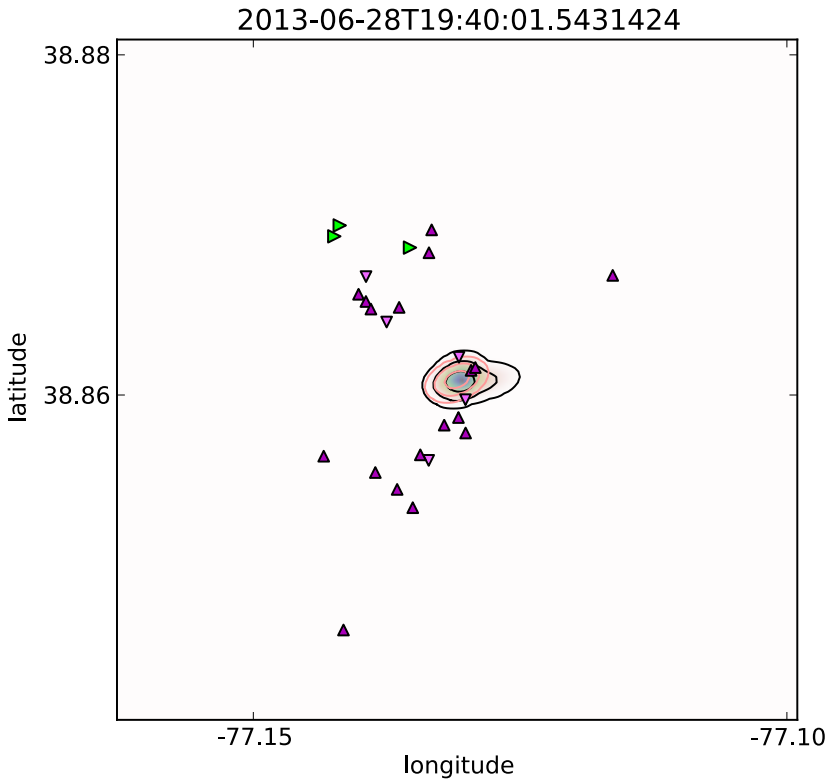

Figure 15: Probability density for fourth pulse of this flash. Black and red contours have same meaning as in all the other figures. Triangles show locations of VHF sources identified in this entire flash. Green triangles occurred within 5 milliseconds of this pulse, and purple triangles are VHF locations more than 5 milliseconds before or after this pulse. The VHF is at the new end of the channel, the low frequency pulse is in the middle of the channel.

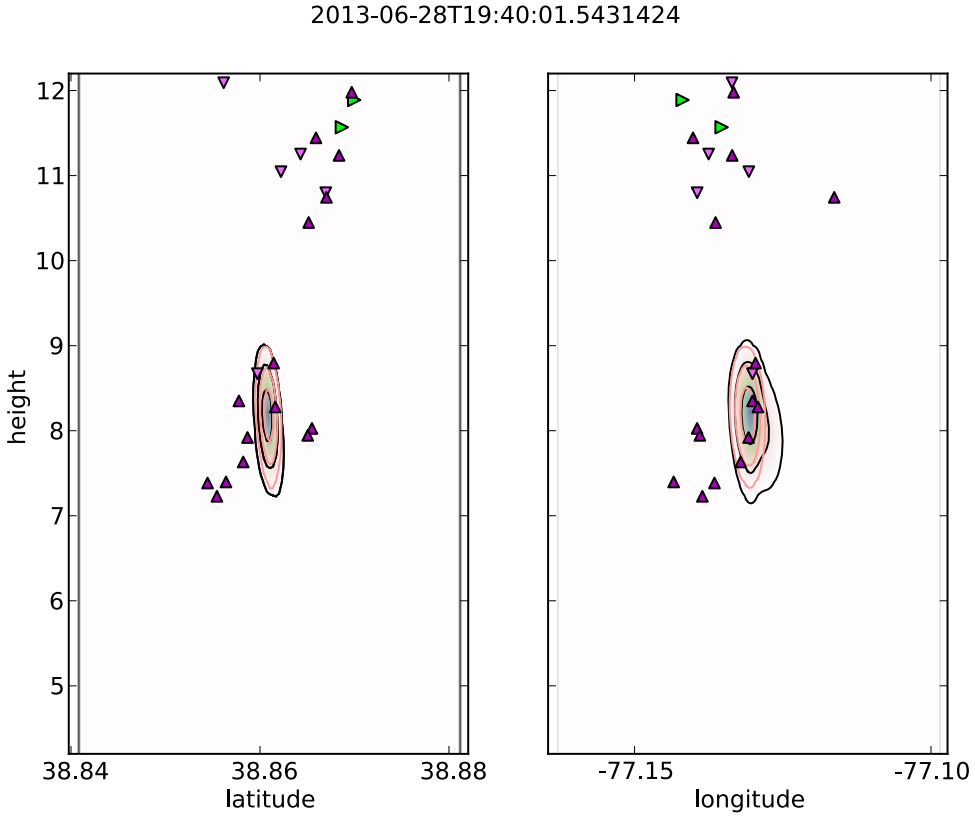

Figure 16: Probability density for height of fourth pulse of this flash. Black and red contours have same meaning as in all the other figures. Triangles show locations of VHF sources identified in this entire flash. Green triangles occurred within 5 milliseconds of this pulse. This is farther east than any previous pulse of this flash. The VHF is in a new portion of the upper end of the channel, the low frequency pulse is in the top of the lower part of the channel.

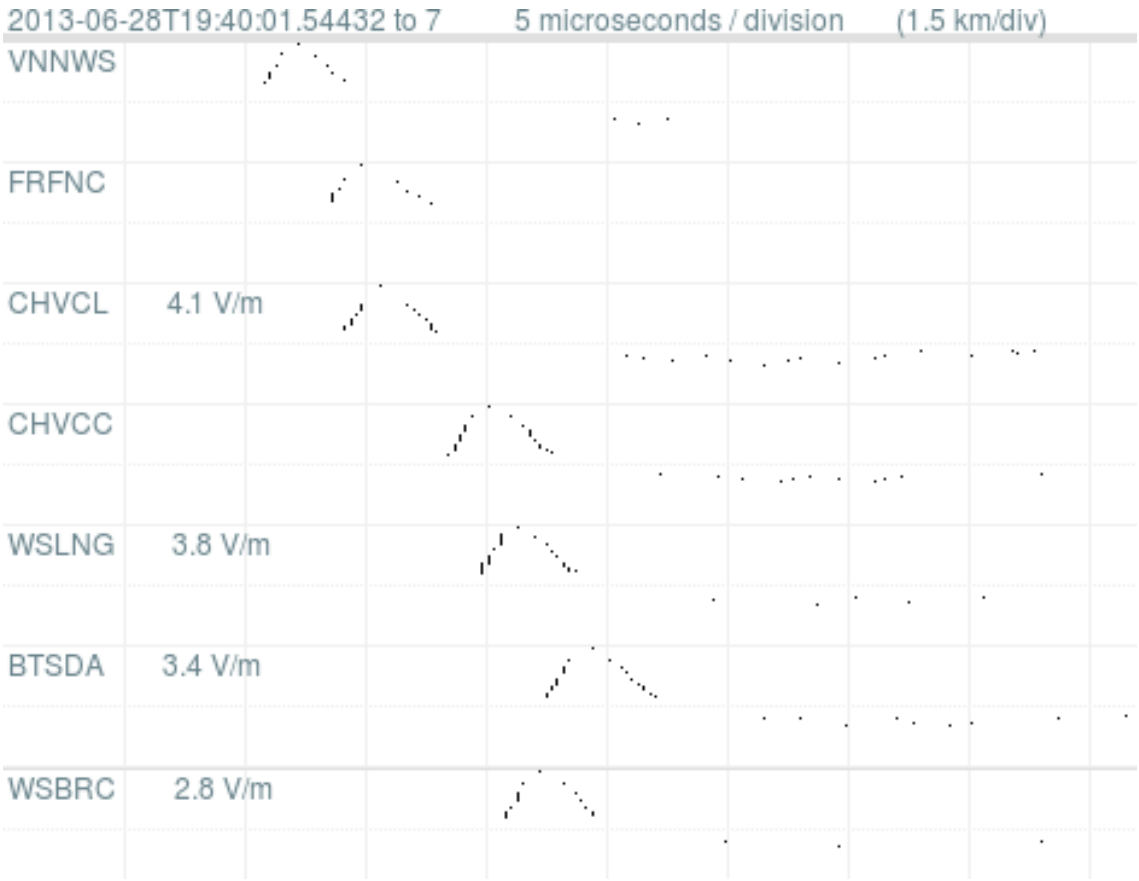

Figure 17: Electric field for fifth pulse.

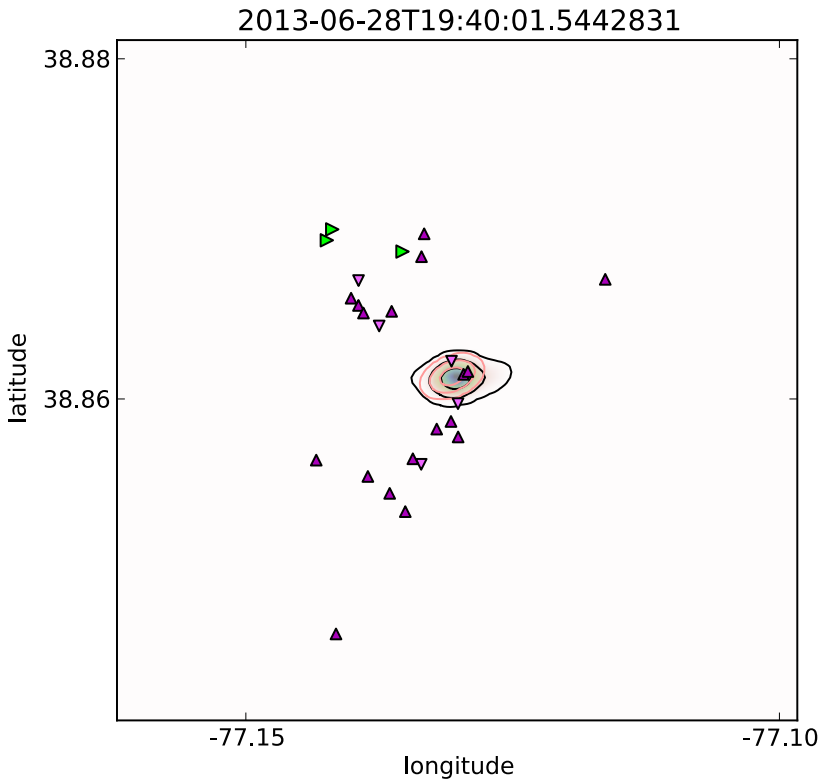

Figure 18: Location of fifth pulse. This happened at almost the same time and the same location as the fourth pulse.

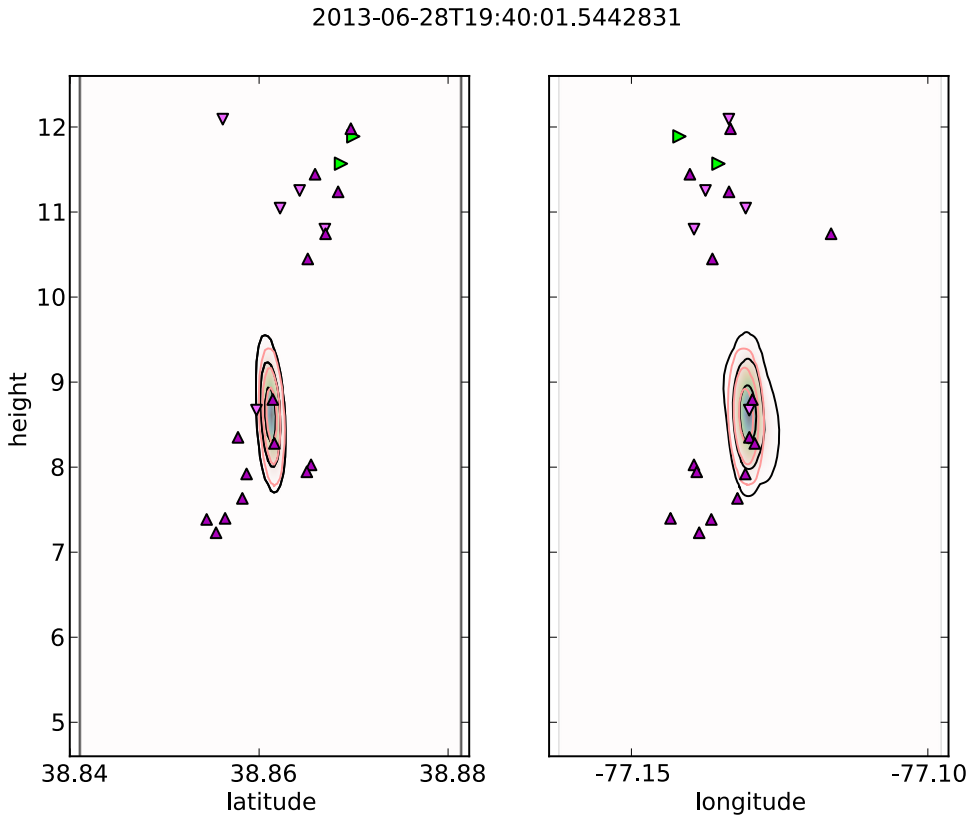

Figure 19: Vertical location of fifth pulse. Almost the same time and location as the fourth pulse.

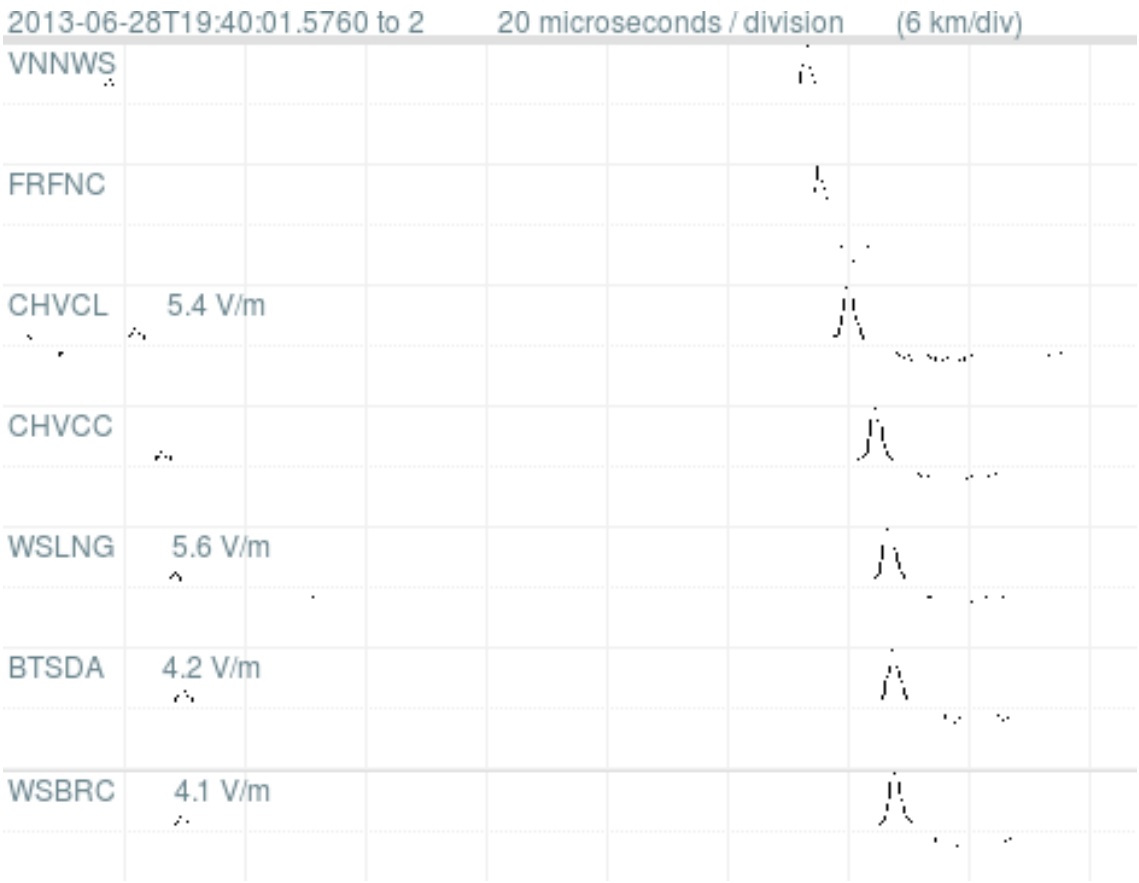

Figure 20: Electric field for sixth pulse.

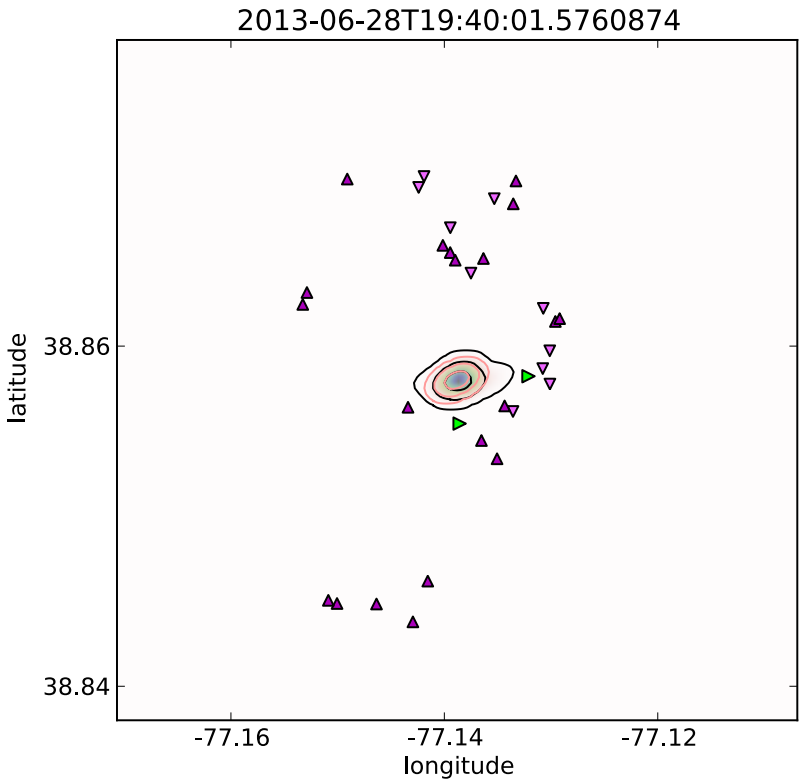

Figure 21: Location of sixth pulse.

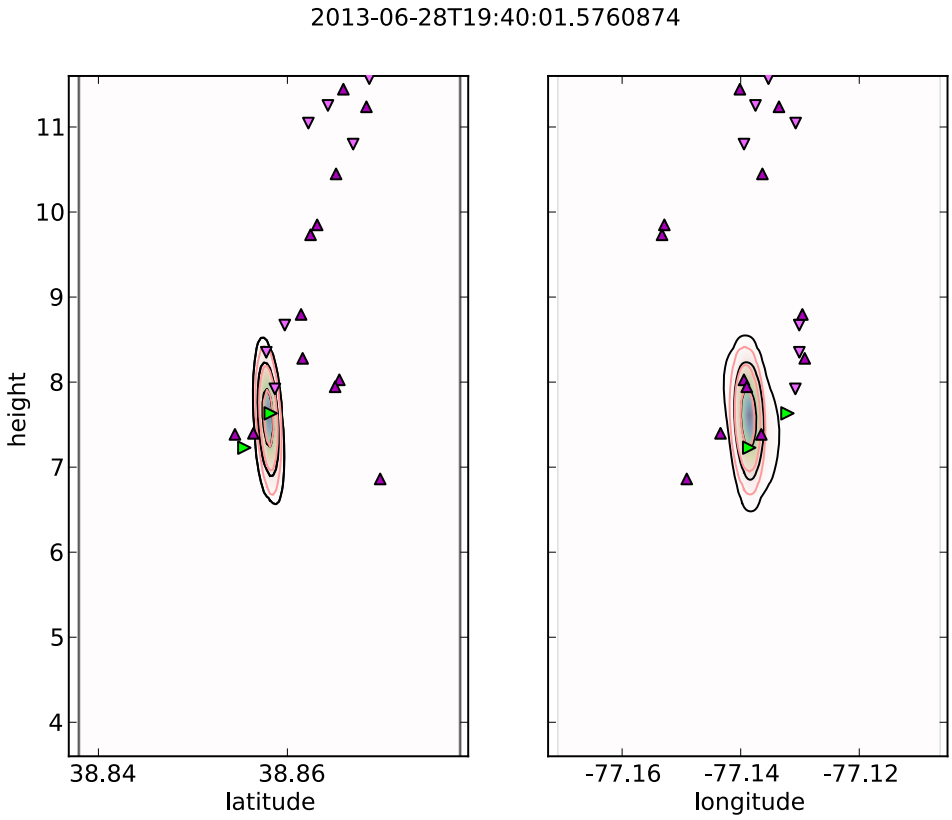

Figure 22: Vertical location of sixth pulse. In the lower section, as is the VHF.

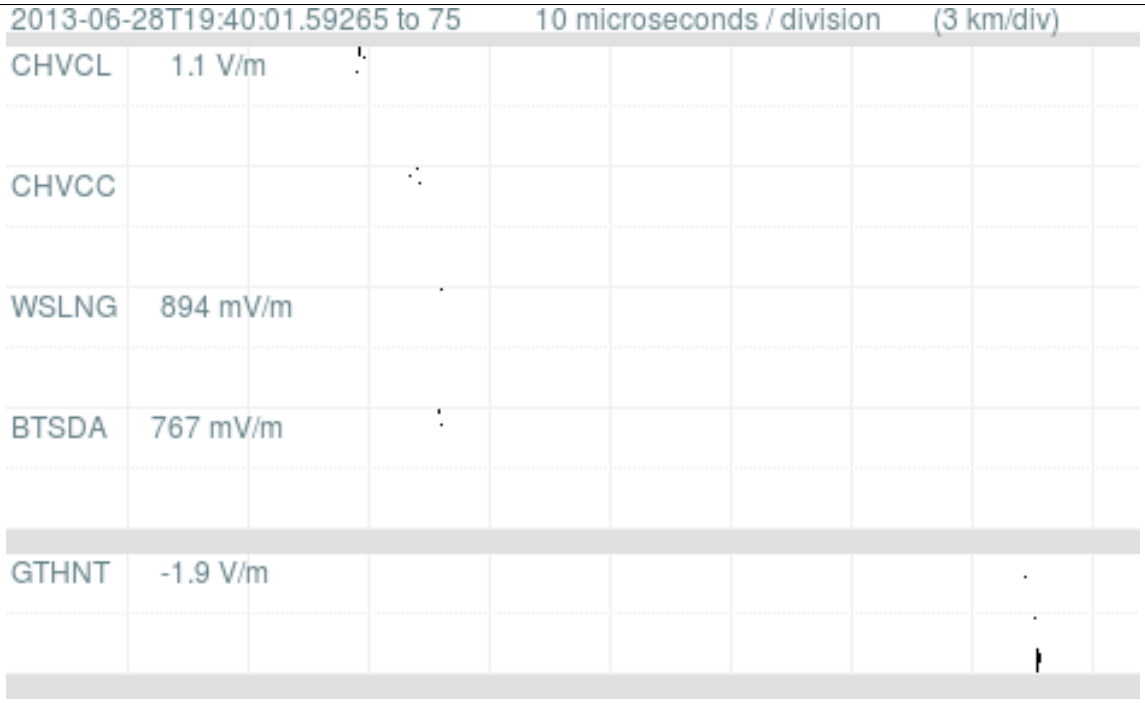

Figure 23: Electric field for seventh pulse. This is barely visible over the noise, and is only seen at 5 sites, so the location errors will probably be large.

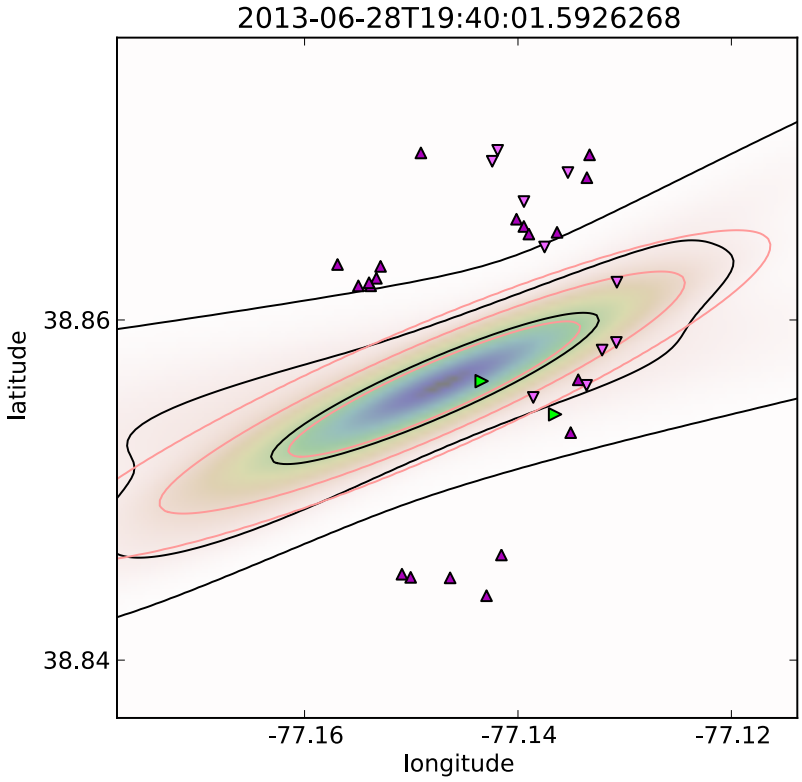

Figure 24: Location of seventh pulse. The location errors are very large; the contours containing 90% and 99% of the total probability density do not fit in the bounds of the plot.

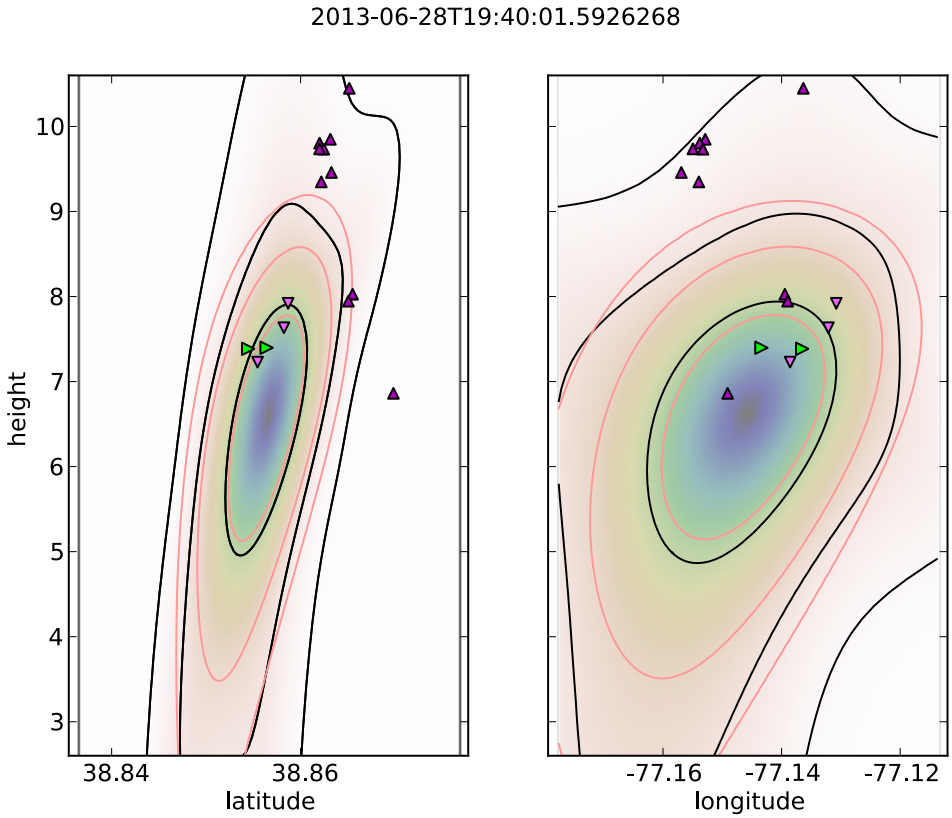

Figure 25: Vertical location of seventh pulse. The maximum probability density is at a plausible height, but that's just a lucky coincidence, the uncertainty is very large.

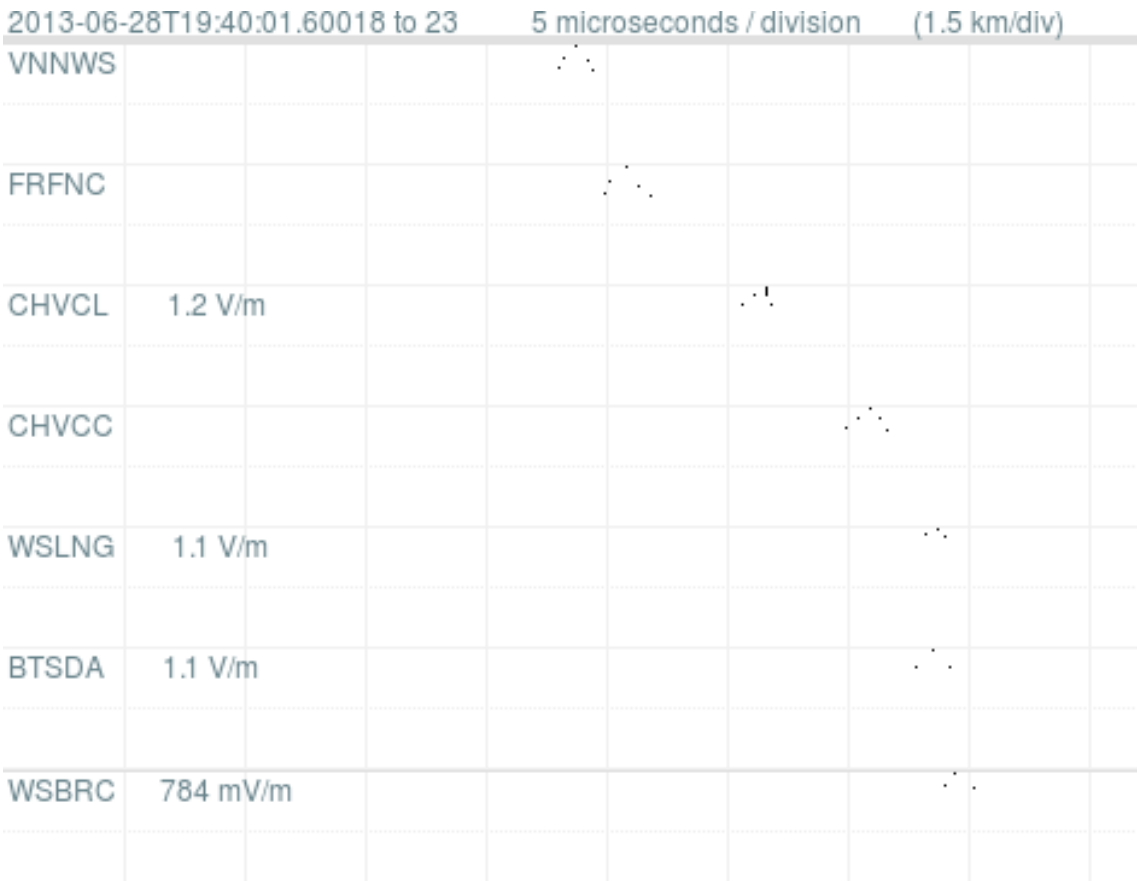

Figure 26: Electric field for eighth pulse.

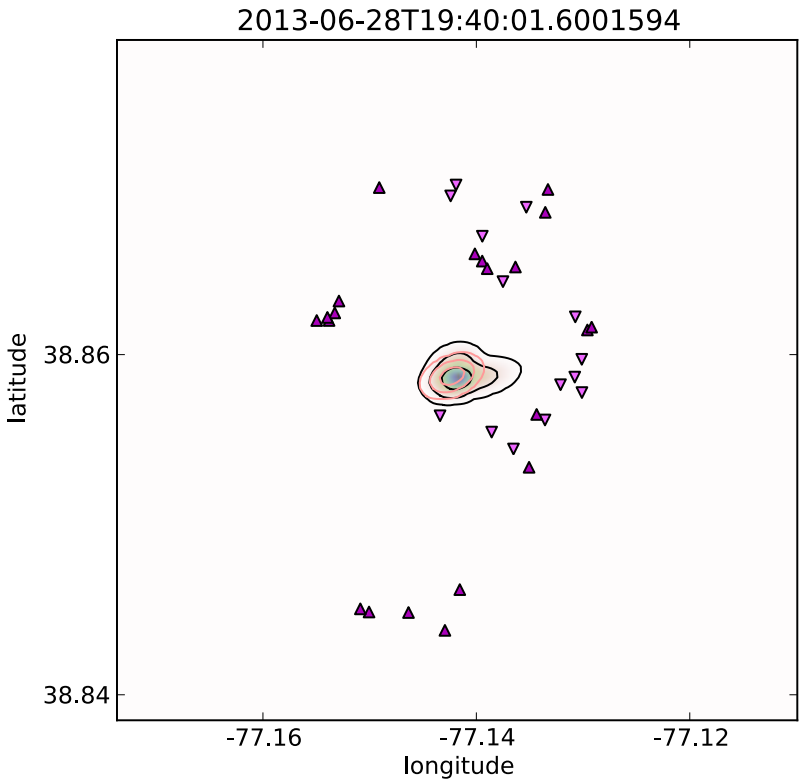

Figure 27: Location of eighth pulse. There is no VHF source within 5 milliseconds of this pulse.

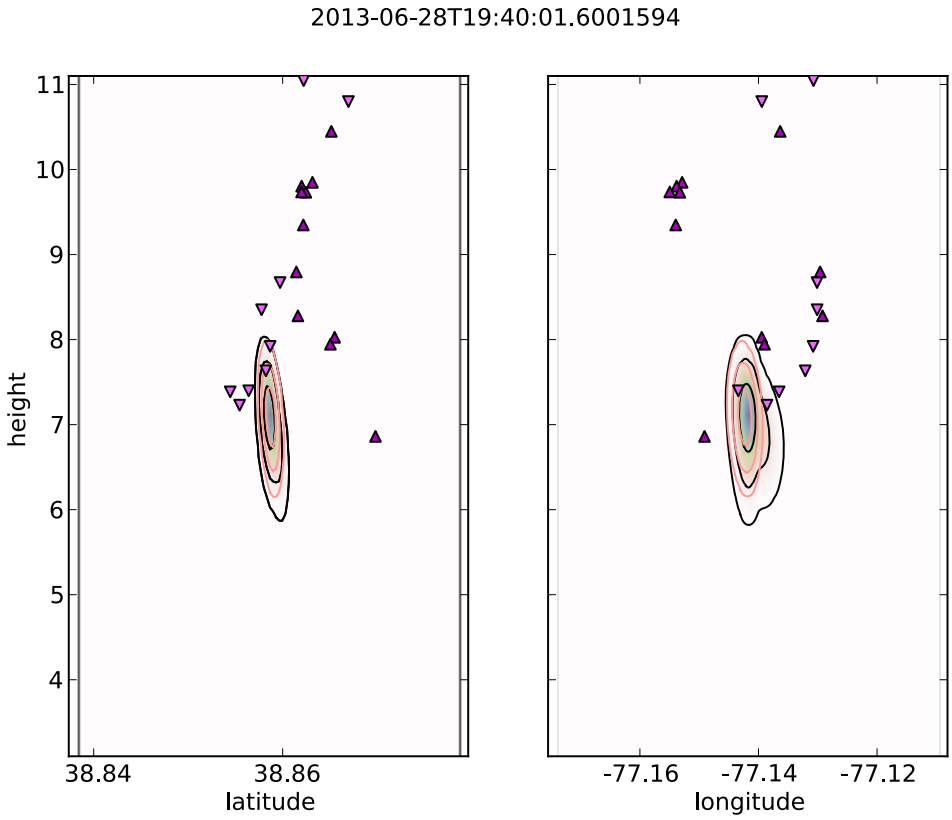

Figure 28: Vertical location of eighth pulse. In the lower section.

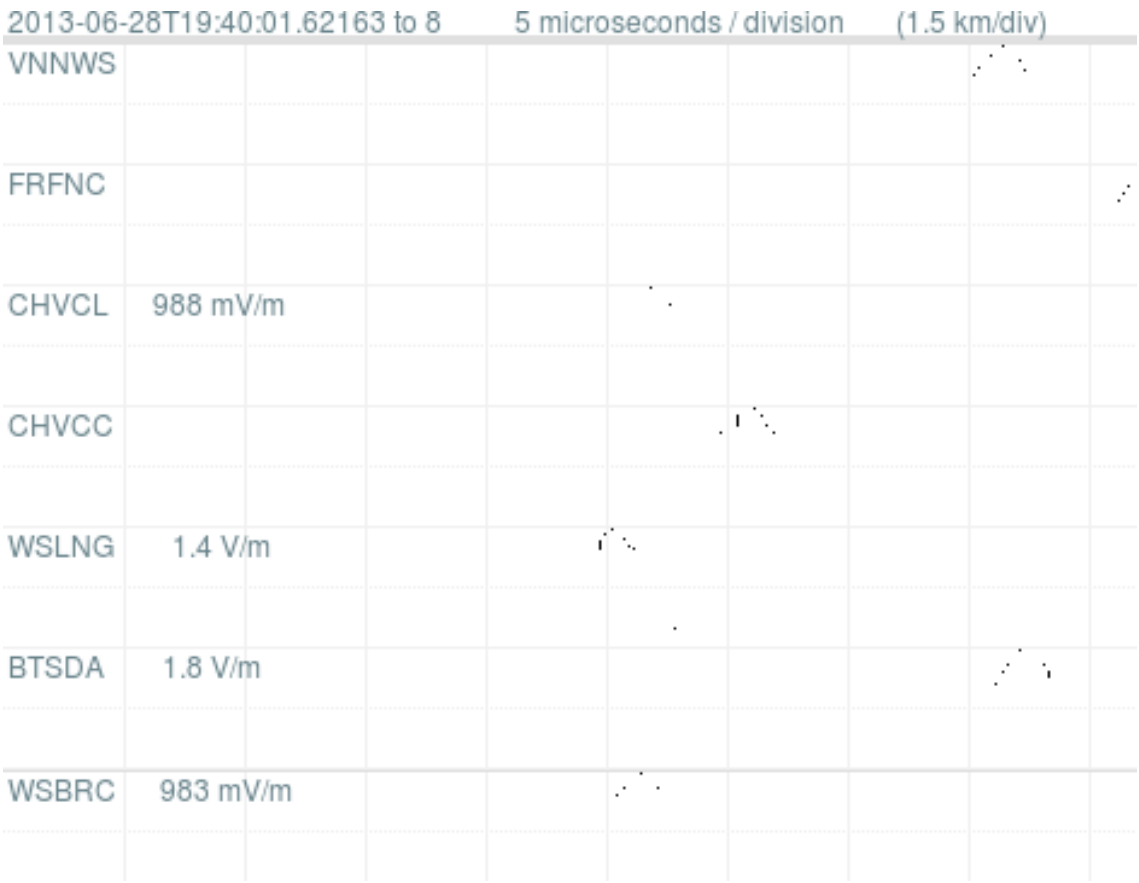

Figure 29: Electric field for ninth pulse.

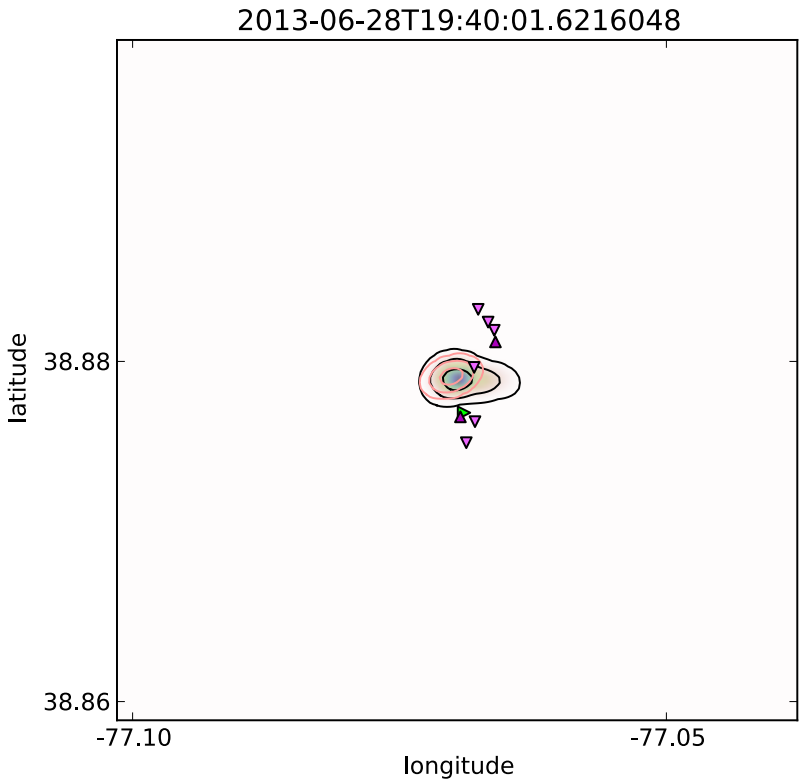

Figure 30: Location of ninth pulse is close to the only VHF source within 5 milliseconds.

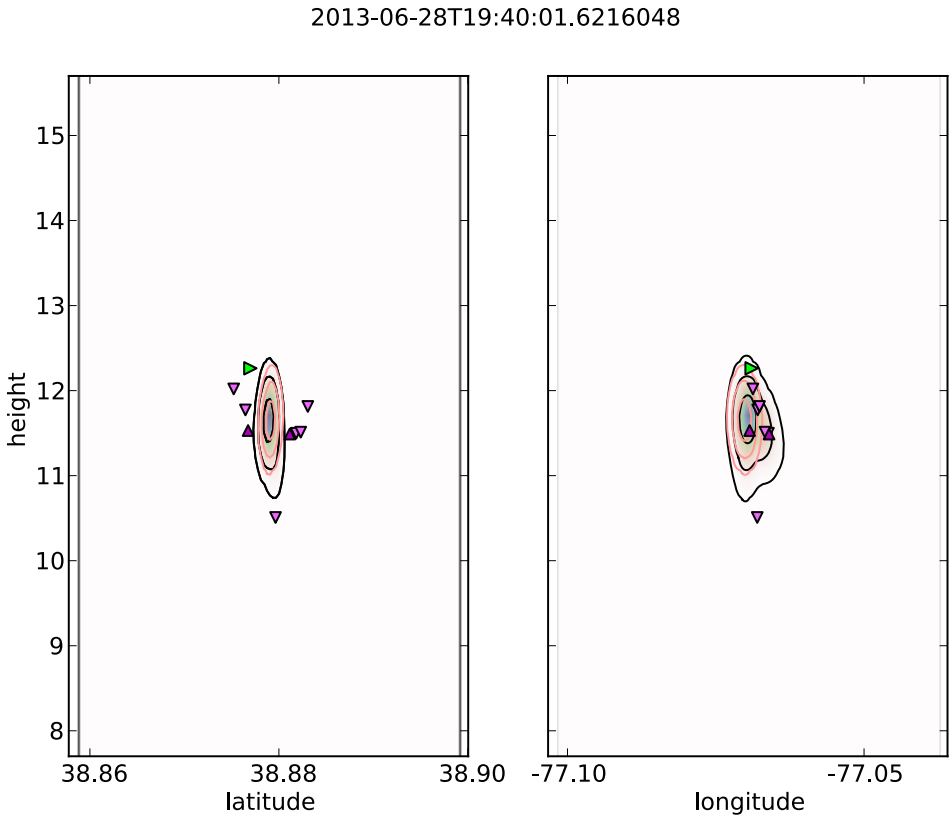

Figure 31: Vertical location of ninth pulse. In the upper section.

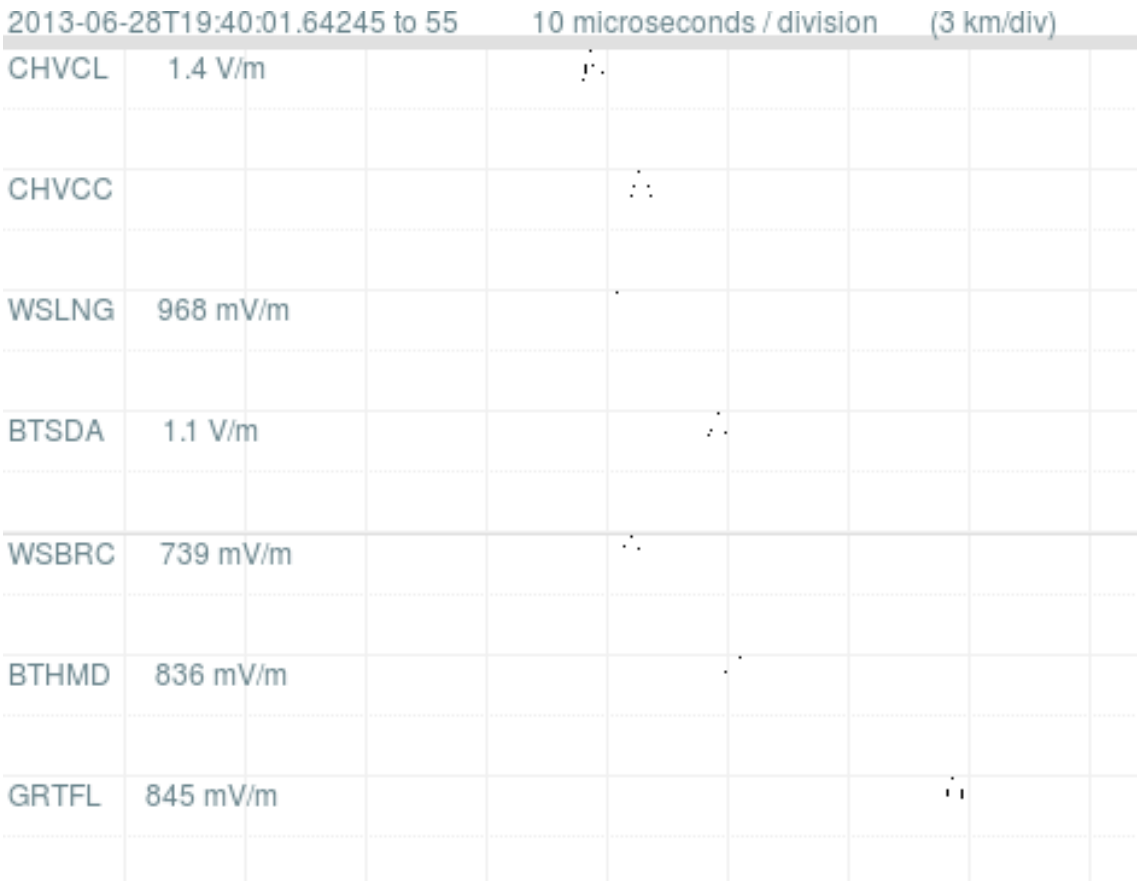

Figure 32: Electric field for tenth pulse.

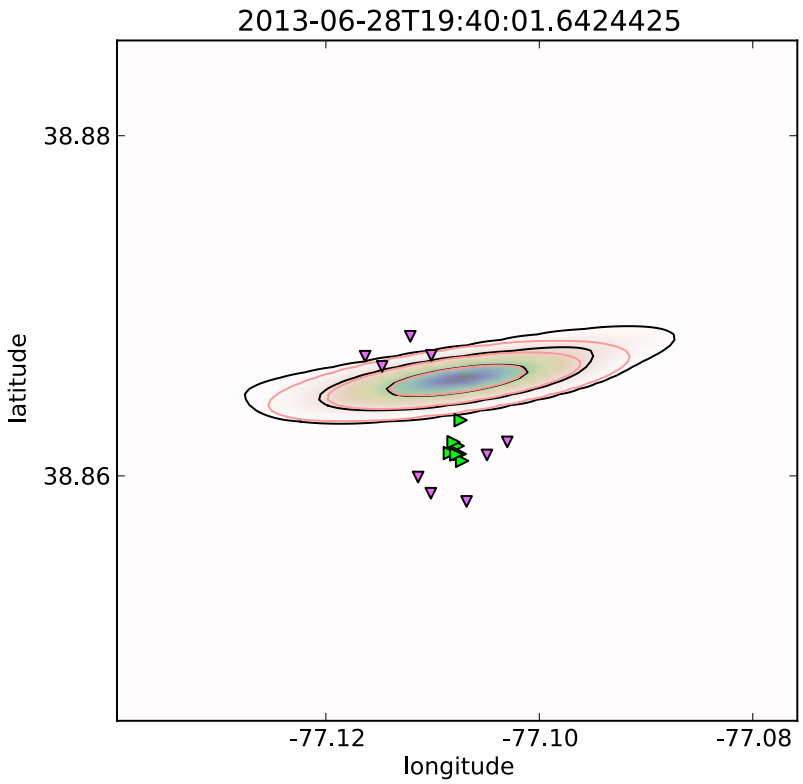

Figure 33: Location of tenth pulse. Quite a bit of longitude uncertainty, but we can still see that this pulse is at the west end of the flash, as opposed to the ninth pulse which was at the east end. The The longitude maximum probability density is close to the VHF pulses within 5 milliseconds (shown in green).

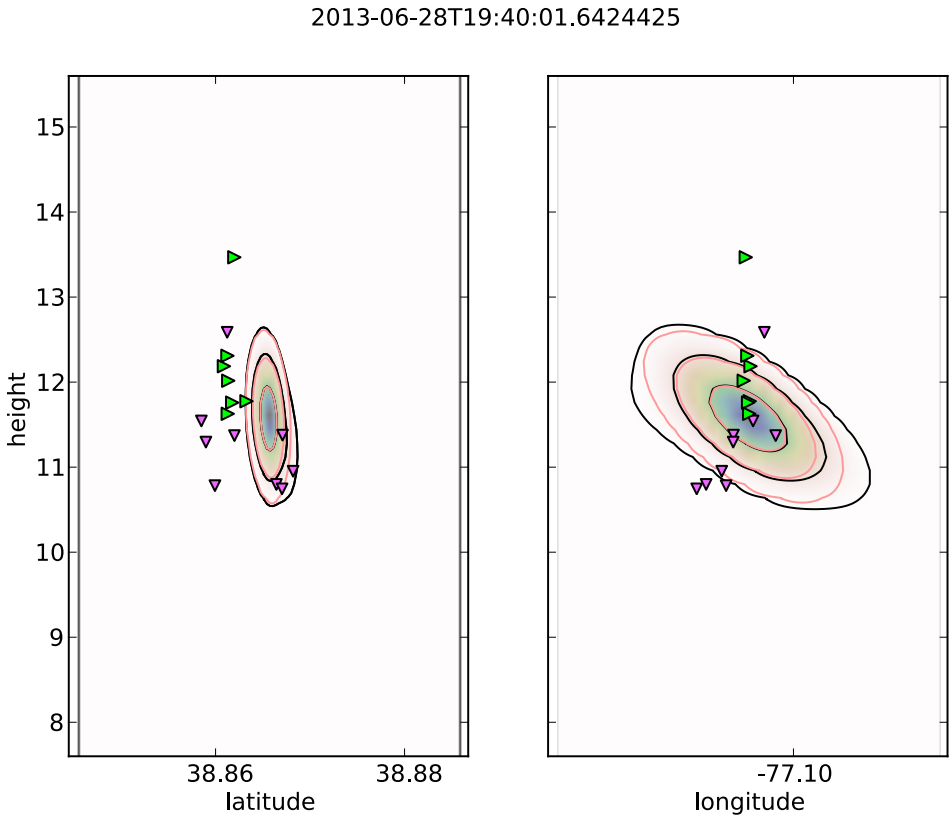

Figure 34: Vertical location of tenth pulse. In the upper section.

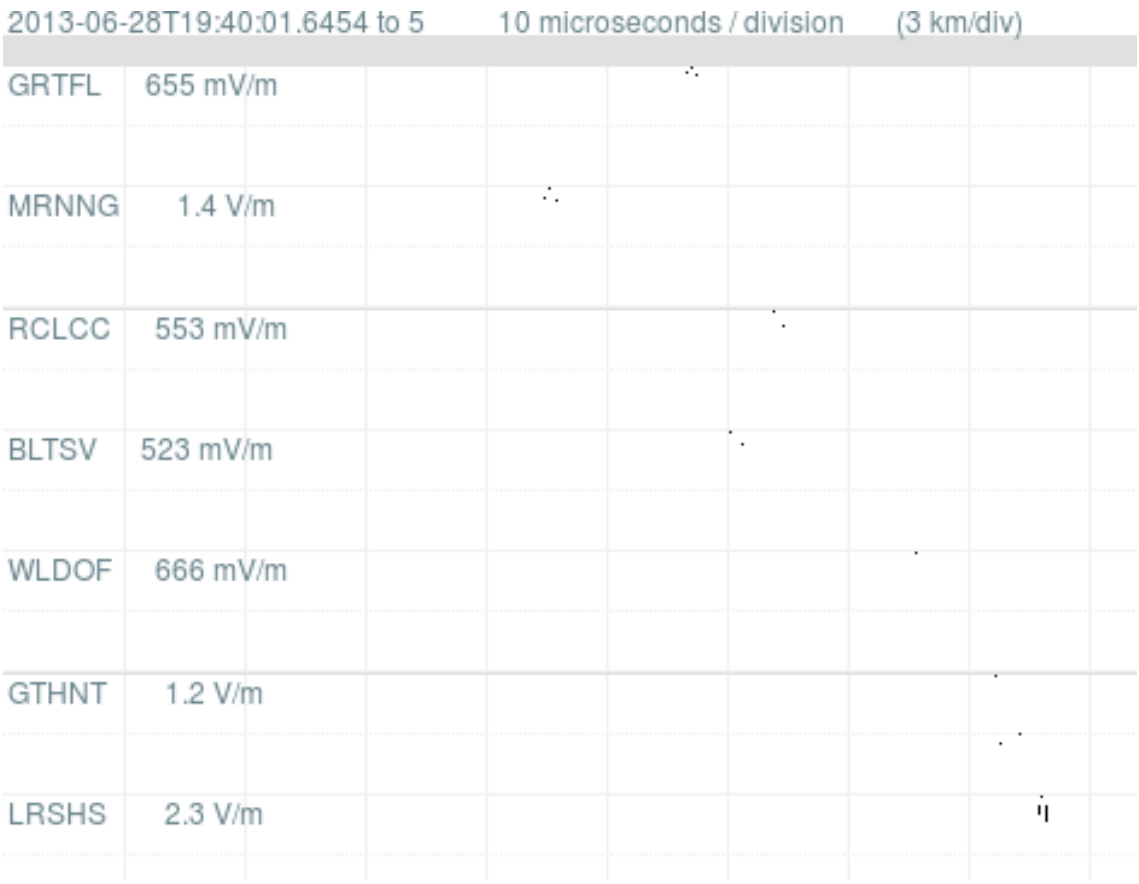

Figure 35: Electric field for eleventh pulse. Barely visible positive pulse. Because it is barely visible, we may have trouble locating it.

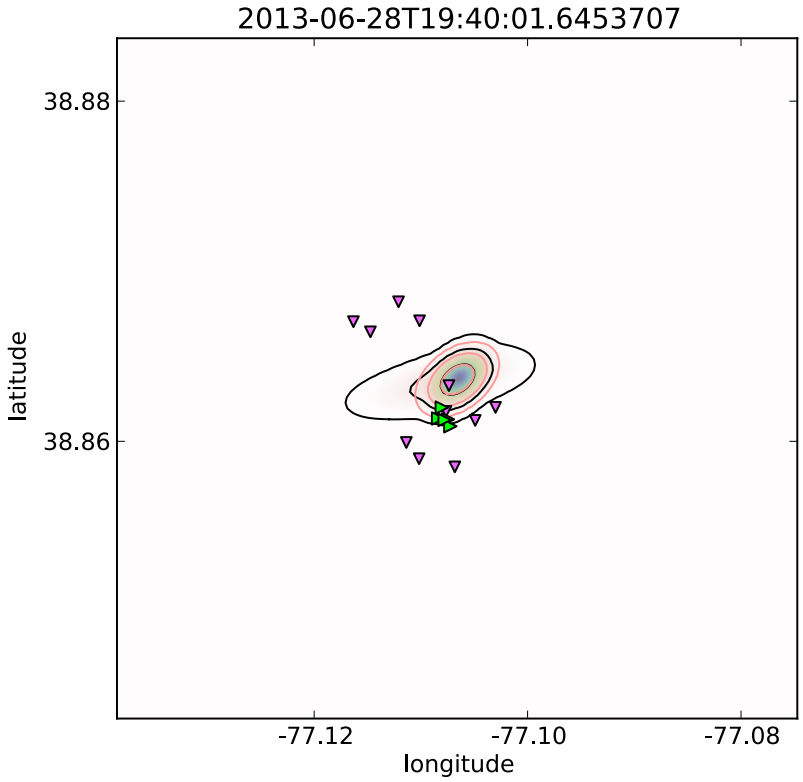

Figure 36: Location of eleventh pulse. VHF is in similar location as previous two pulses, all showing new channel extending upward. The lower frequency pulse is lower and a bit farther north, in agreement with the location of the previous two lower frequency pulses. The lower frequency pulse location is between the VHF and the lower channel illuminated 100 milliseconds earlier.

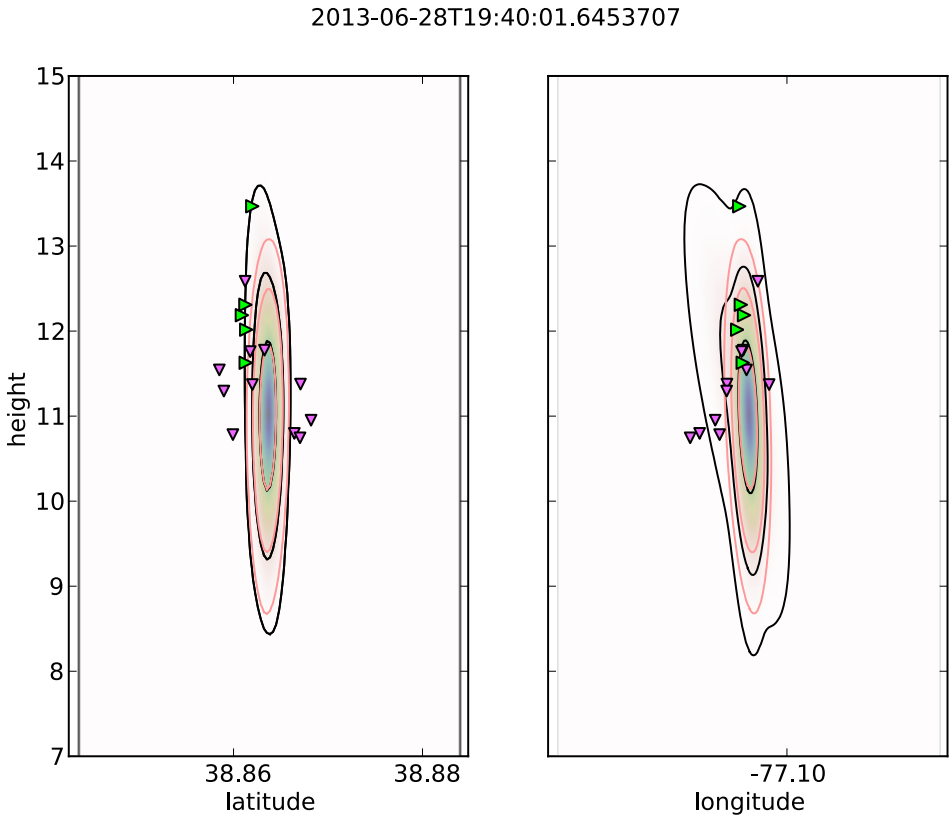

Figure 37: Vertical location of eleventh pulse. Similar to previous two pulses.

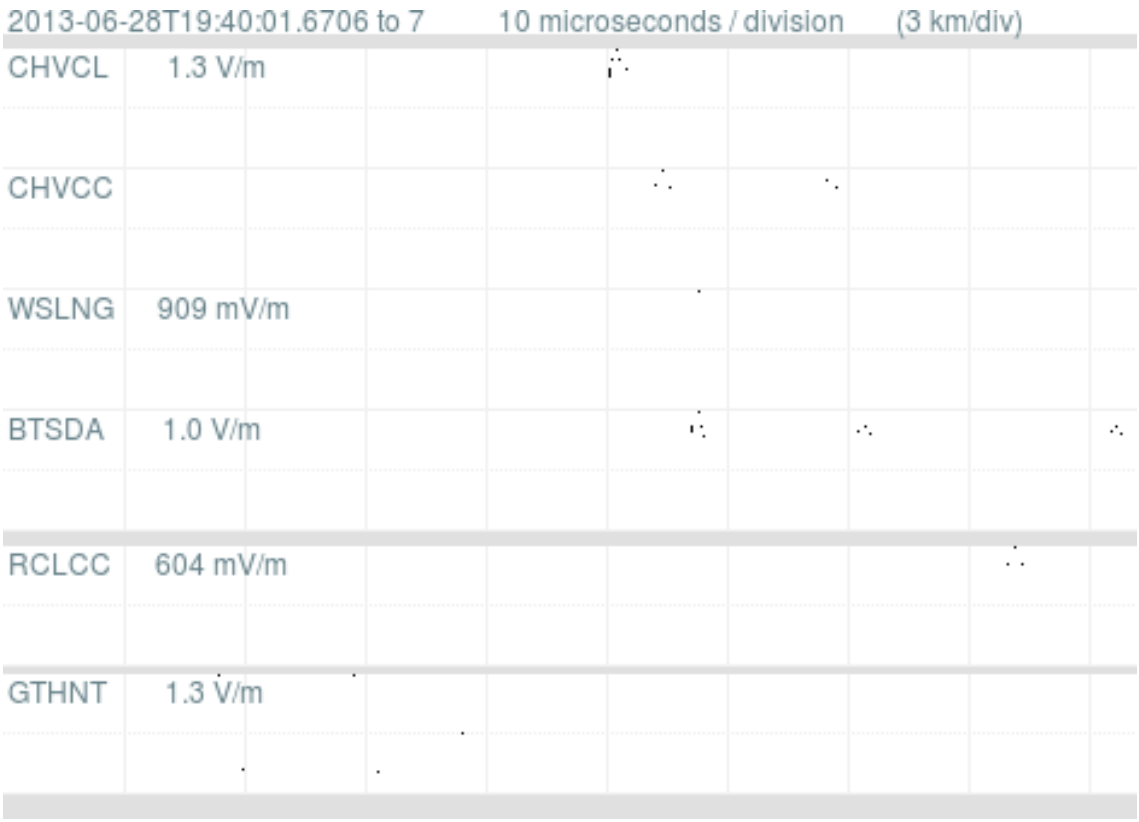

Figure 38: Electric field for twelth pulse. Nice triplet of positive pulses, 15 to 20 microseconds apart and each about one microsecond wide. No VHF sources close to this time.

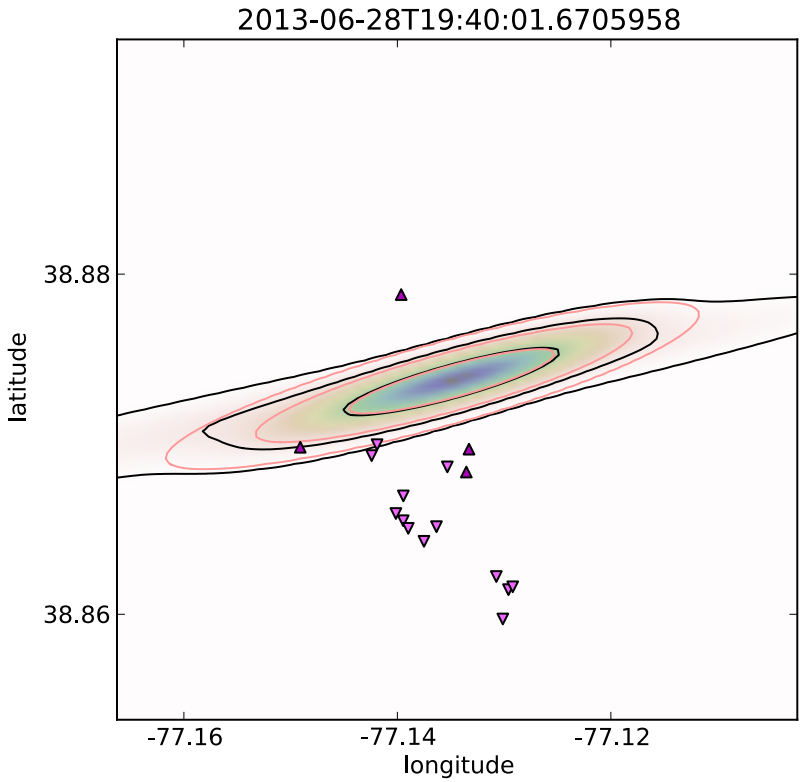

Figure 39: Location of twelth pulse. Near old channel, but not exactly over any old VHF location. There was no VHF radiation within 5 milliseconds of this pulse train.

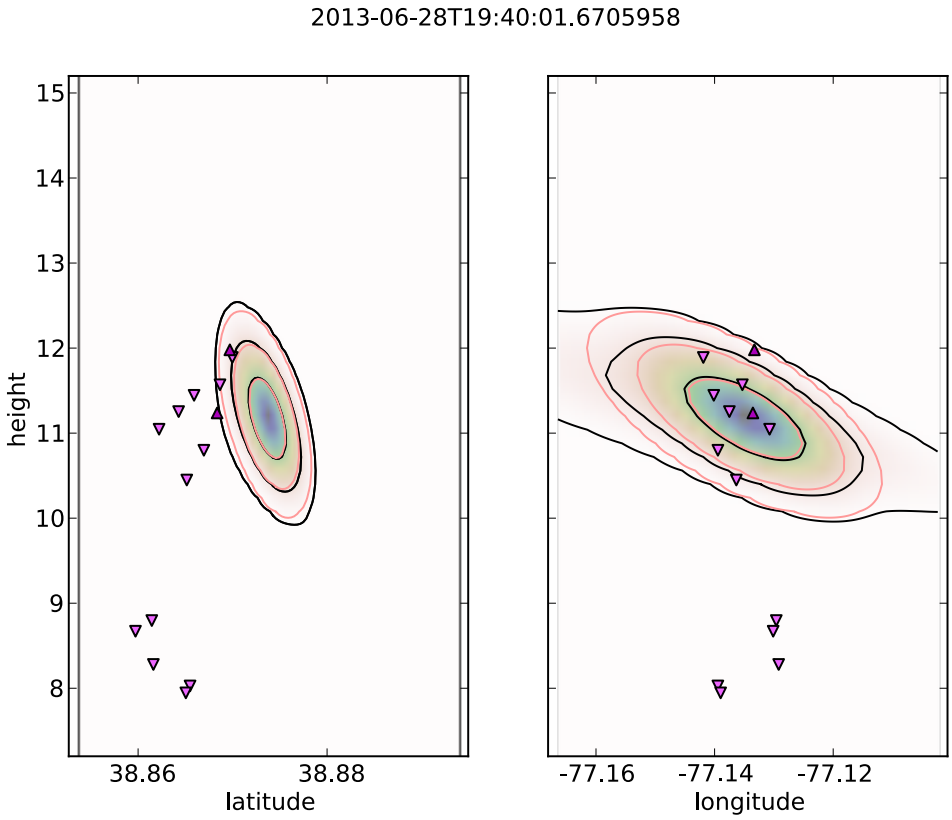

Figure 40: Vertical location of twelth pulse. Near old channel sections. No VHF pulses at this time to compare to.

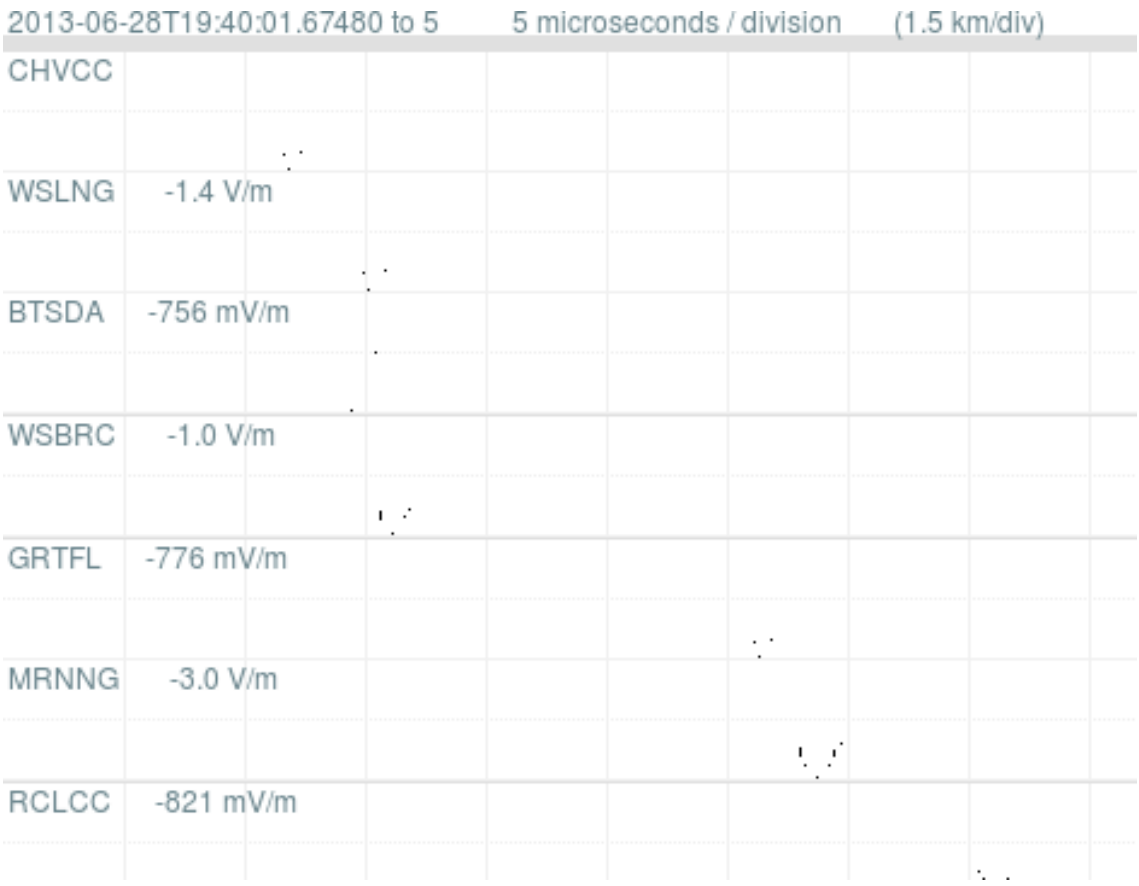

Figure 41: Electric field for thirteenth pulse. This is the first negative radiation field pulse we saw in this flash. There is nearby VHF radiation.

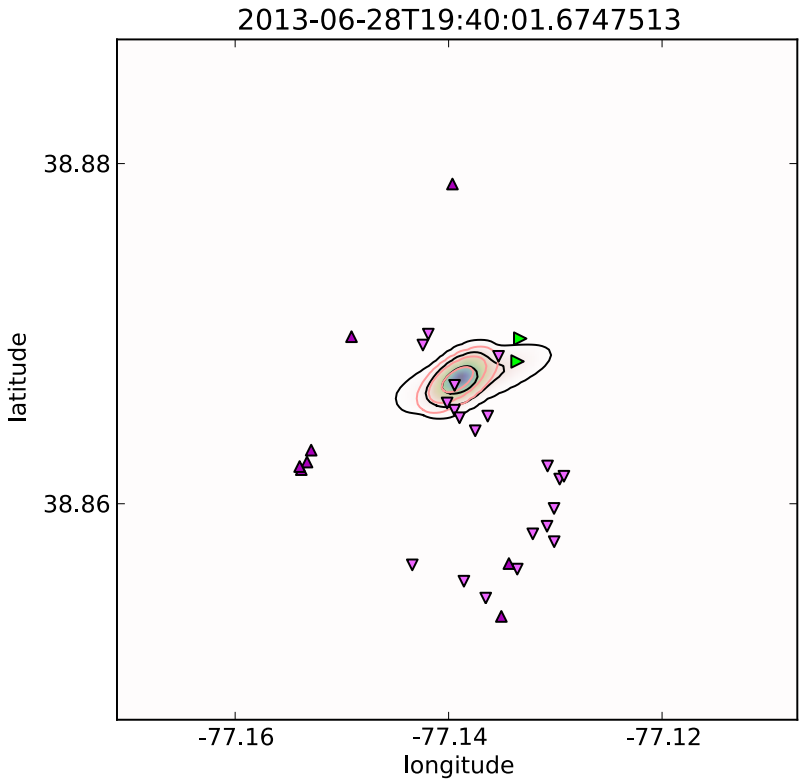

Figure 42: Location of thirteenth pulse. Near the VHF radiation within 5 milliseseconds, but a bit closer to old channel sections, perhaps ”behind” the VHF.

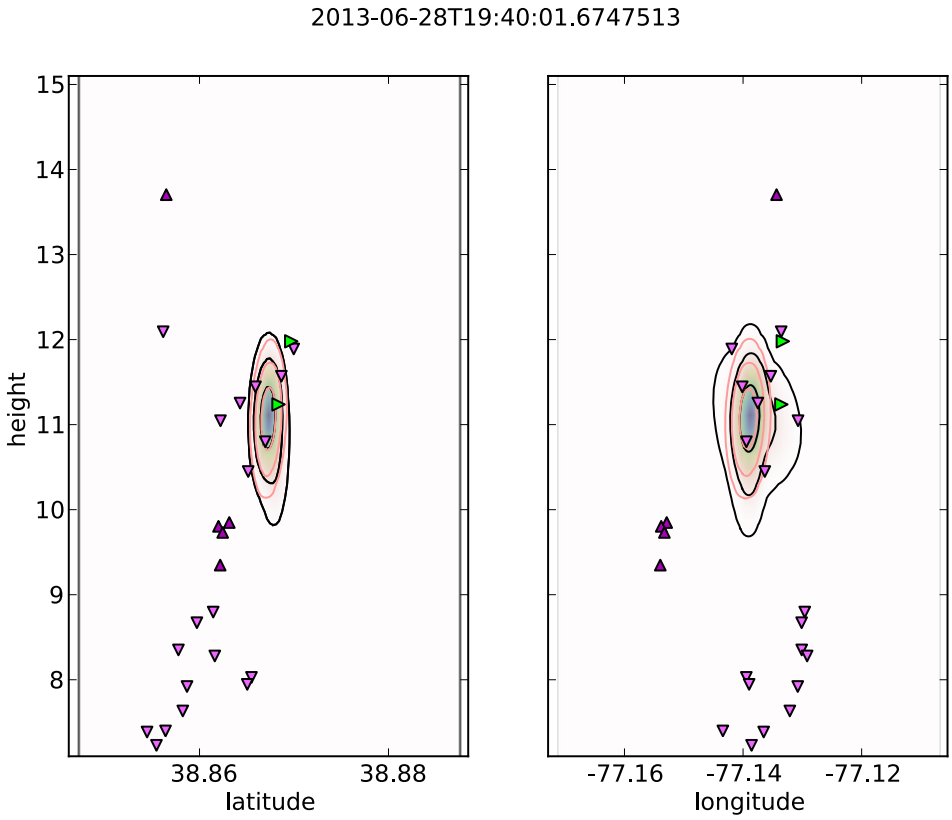

Figure 43: Vertical location of thirteenth pulse. Near the VHF radiation within 5 milliseseconds.

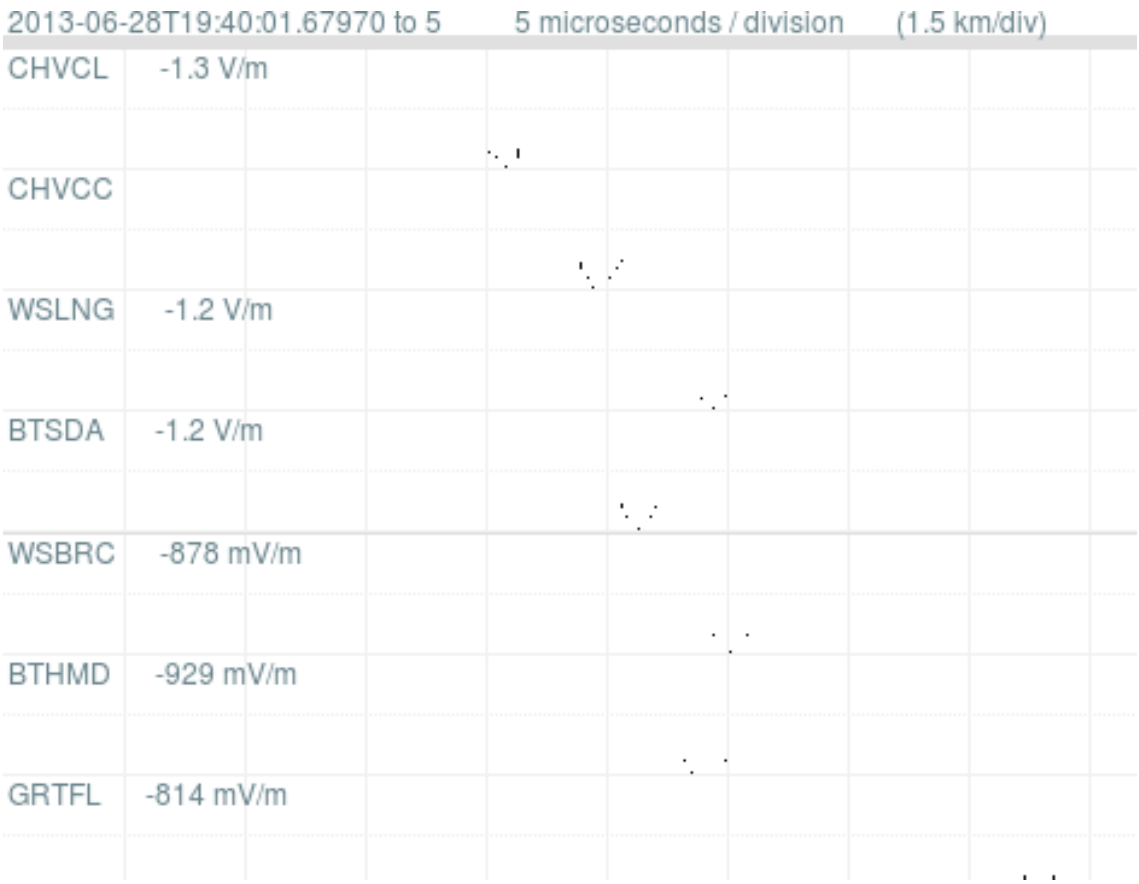

Figure 44: Electric field for fourteenth pulse. This is the second negative radiation field pulse we saw in this flash, about 5 milliseconds after the first one. There is nearby VHF radiation.

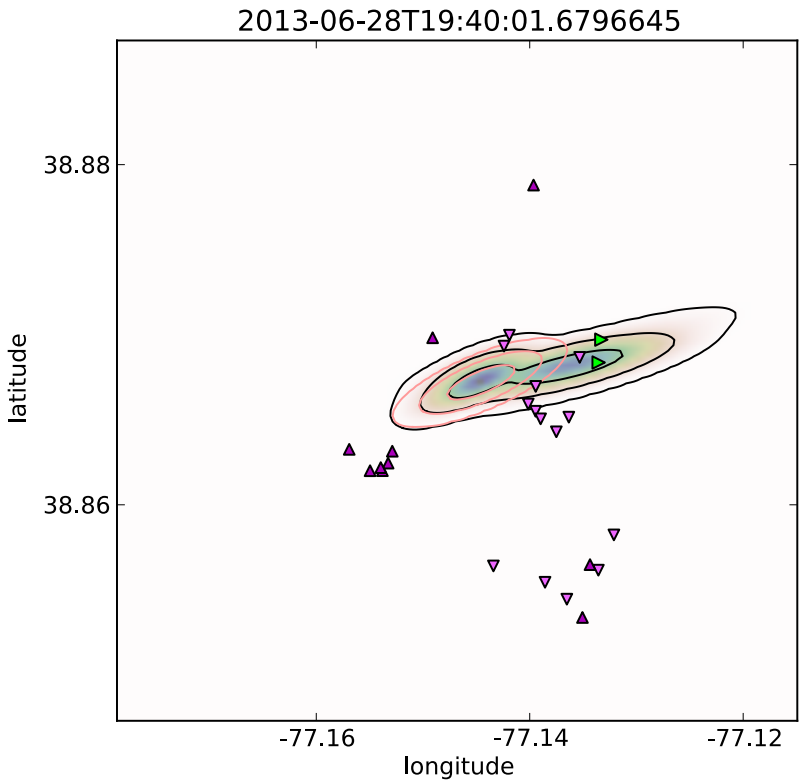

Figure 45: Location of fourteenth pulse. Near the VHF radiation within 5 milliseseconds. The probability density has two distinct local maxima. The contours containing 50%, 90%, and 99% of the total probability enclose both maxima. Had we assumed gaussian timing errors (red ellipses), we would have seen only one of these two local maxima.

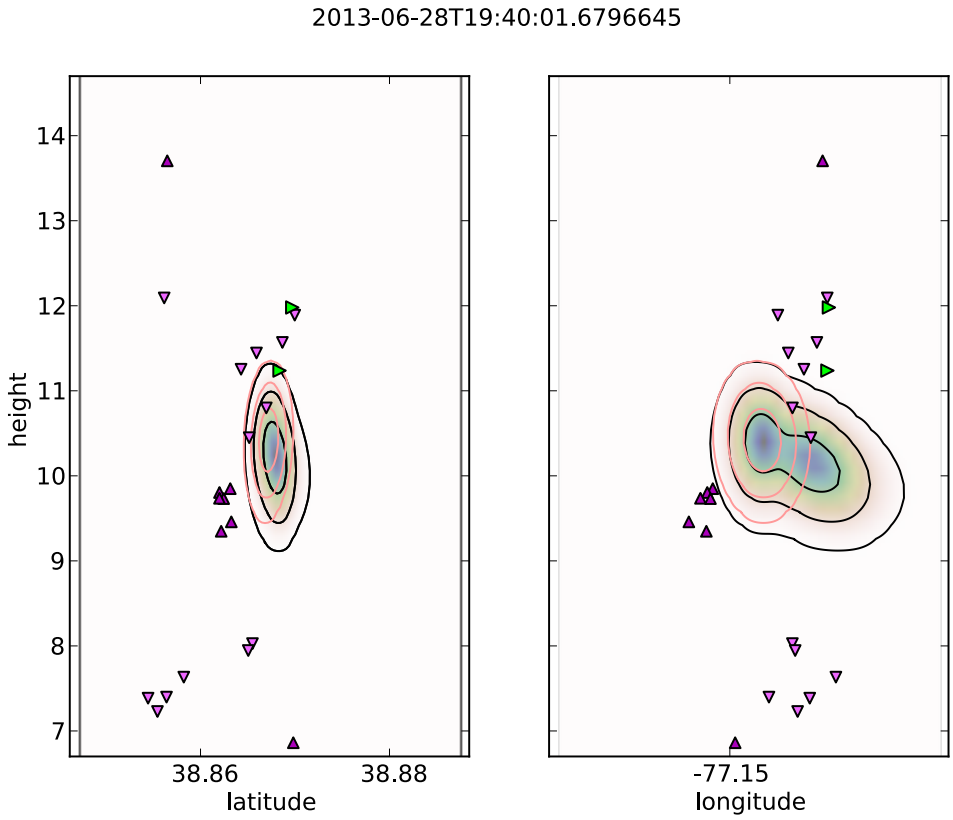

Figure 46: Vertical location of fourteenth pulse. The LF is a bit below the VHF, toward but not on top of old VHF sources.

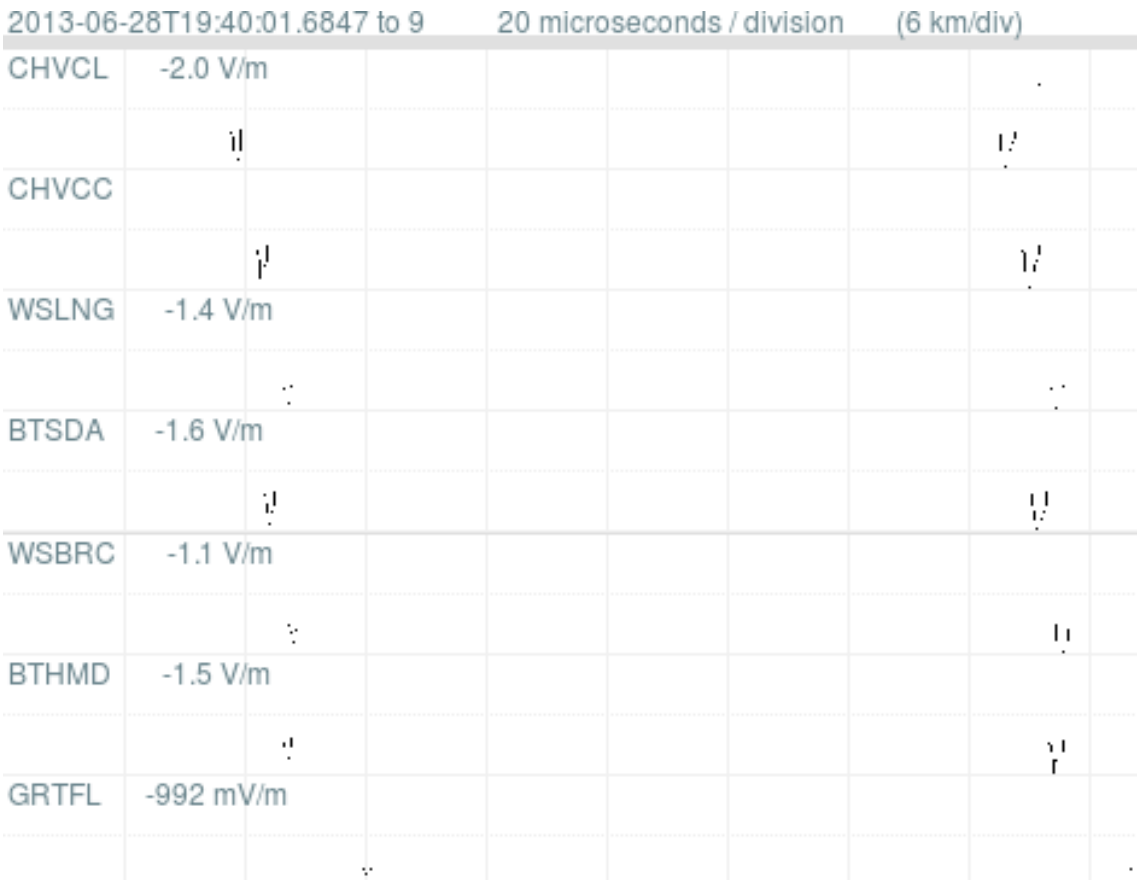

Figure 47: Electric field for fifteenth pulse. This is the third negative radiation field pulse we saw in this flash, each 5 milliseconds after the previous one. There is no VHF radiation within 5 milliseconds of this pulse.

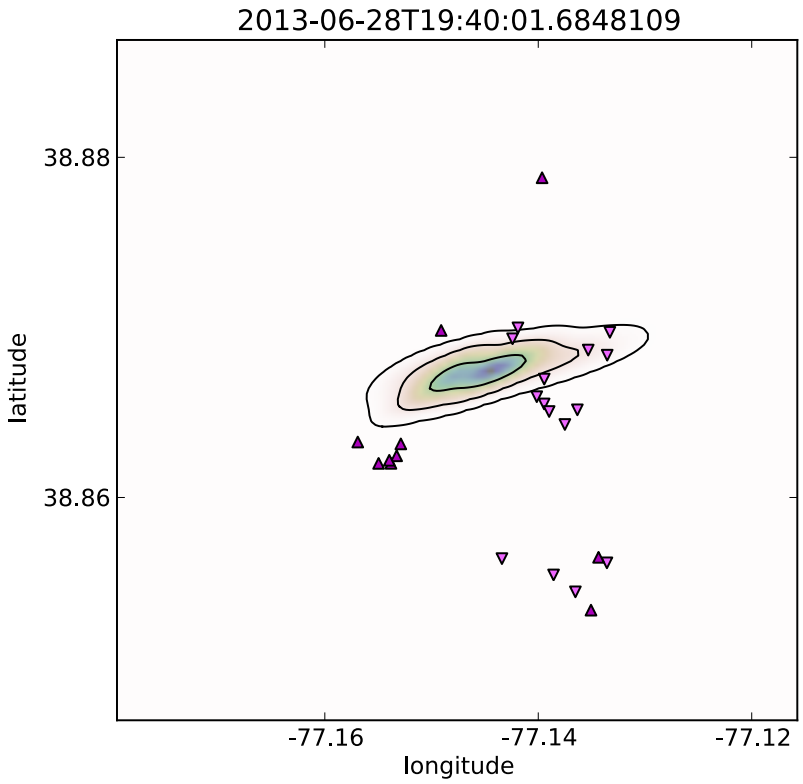

Figure 48: Location of fifteenth pulse.

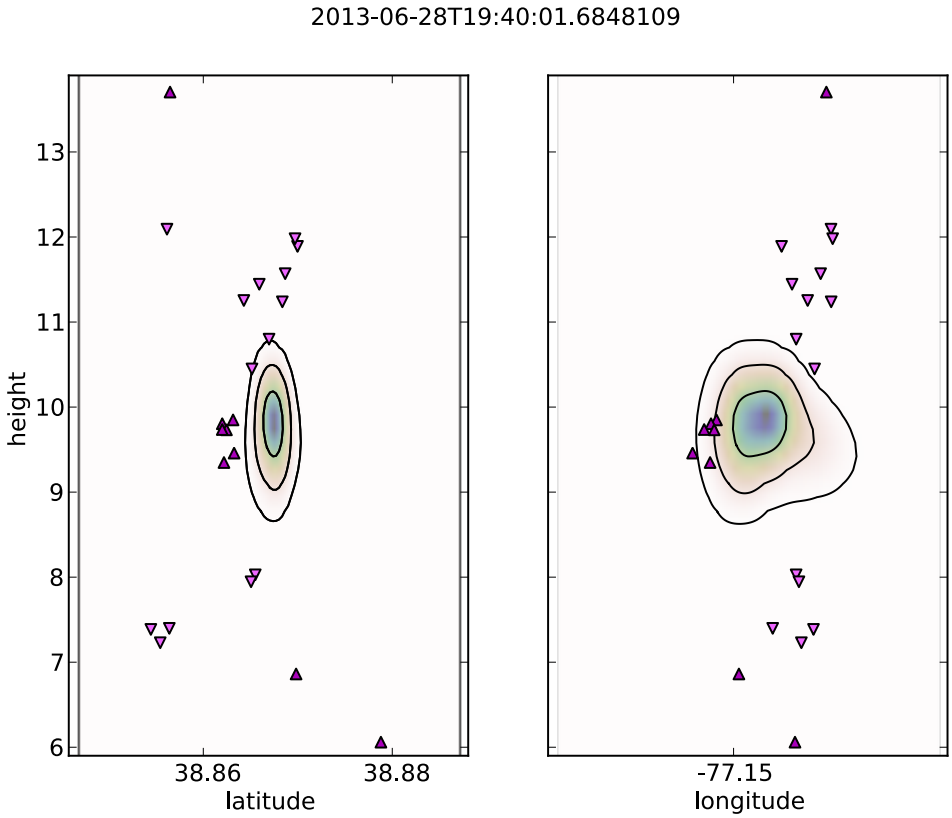

Figure 49: Vertical location of fifteenth pulse. There is no VHF radiation within 5 milliseconds of this pulse. The LF pulse is located between previous upper level and previous lower level VHF sources.

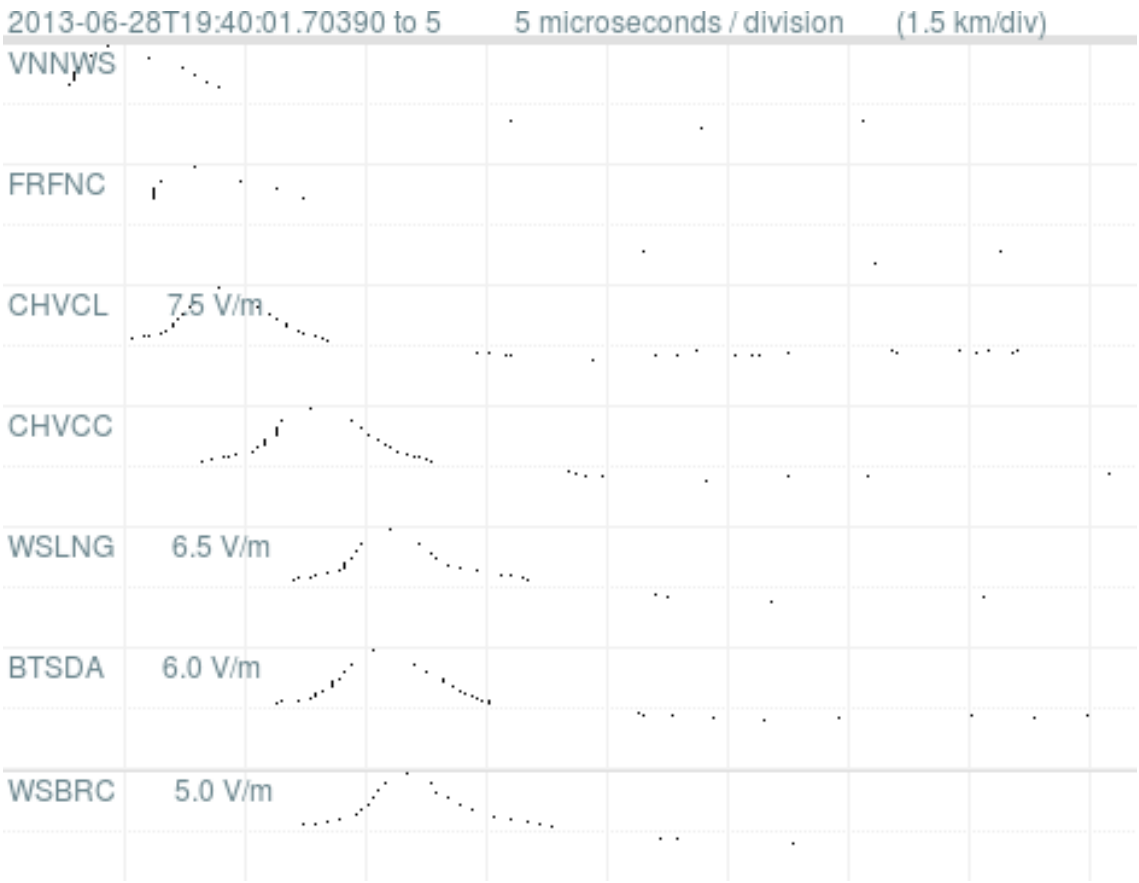

Figure 50: Electric field for sixteenth pulse. Positive radiation field, as were all pulses so far except the previous 3.

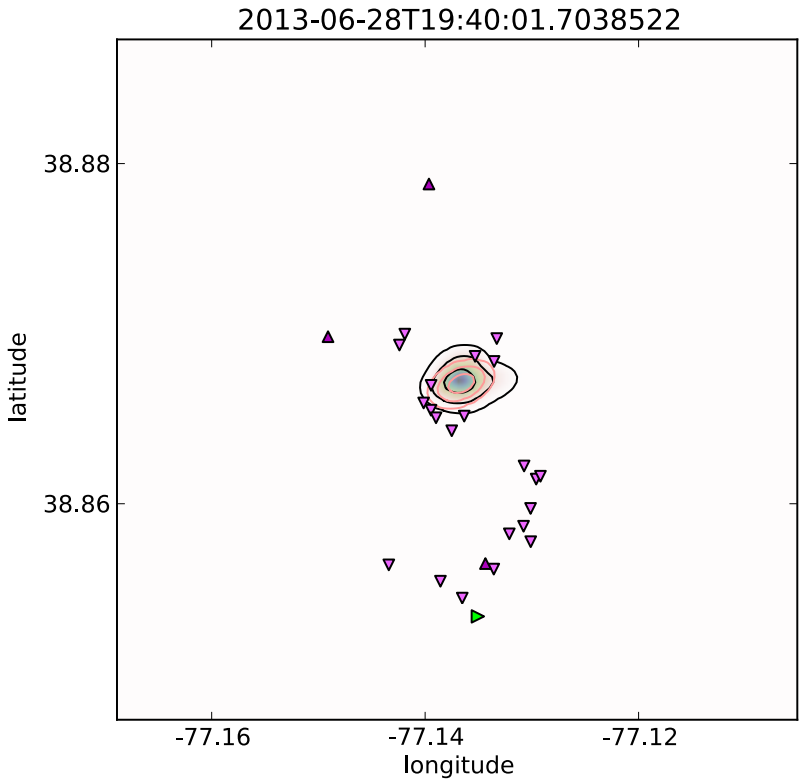

Figure 51: Location of sixteenth pulse. In the middle of previously illuminated channel sections, but far from the VHF within 5 milliseconds. This pulse occurred several hundred microseconds before the VHF.

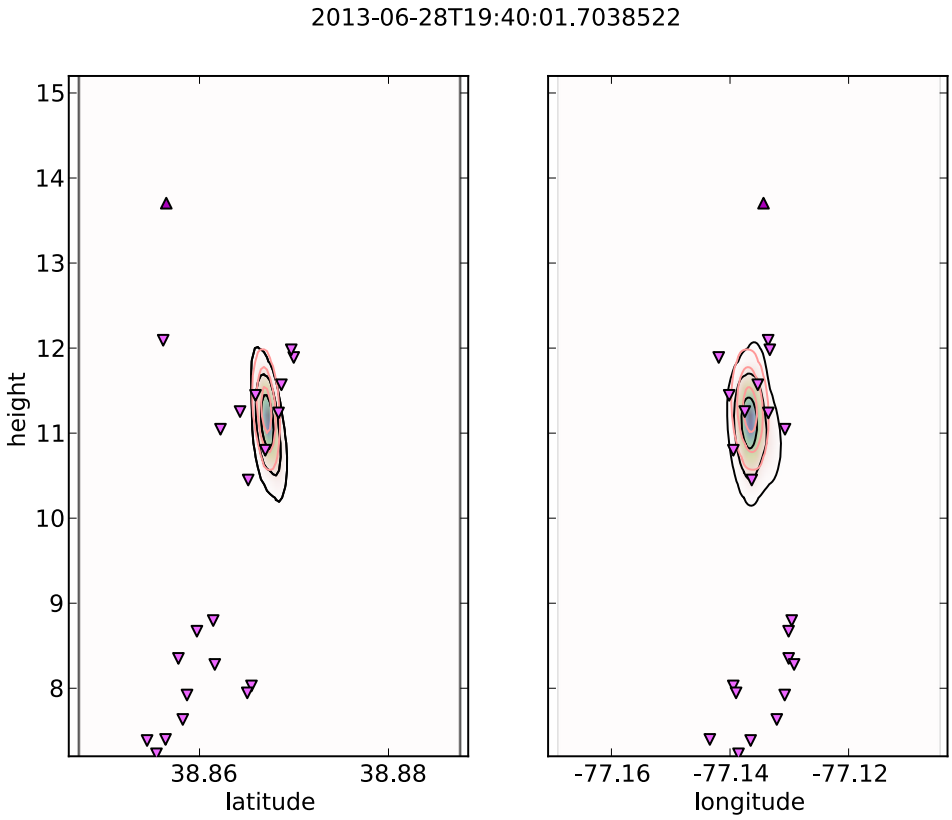

Figure 52: Vertical location of sixteenth pulse.

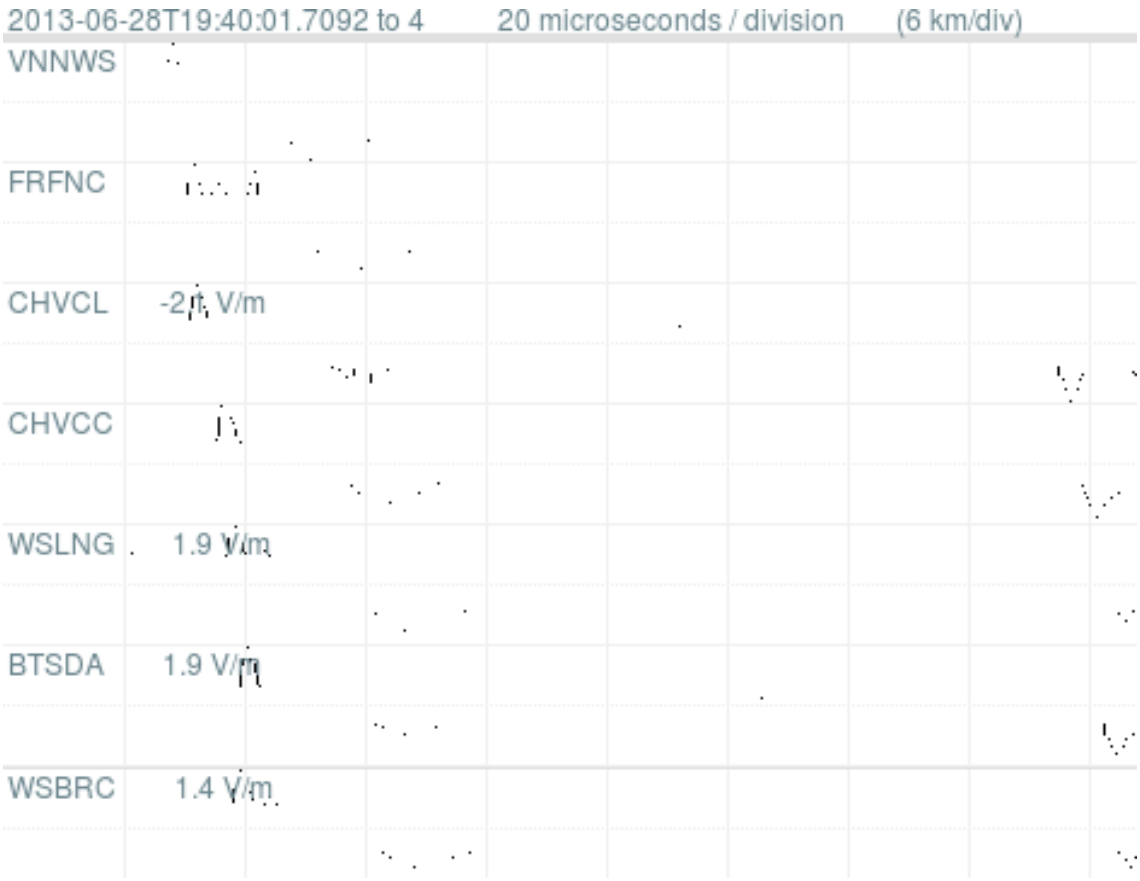

Figure 53: Electric field for seventeenth pulse. Positive radiation field, the negative field pulse soon after is at a different location.

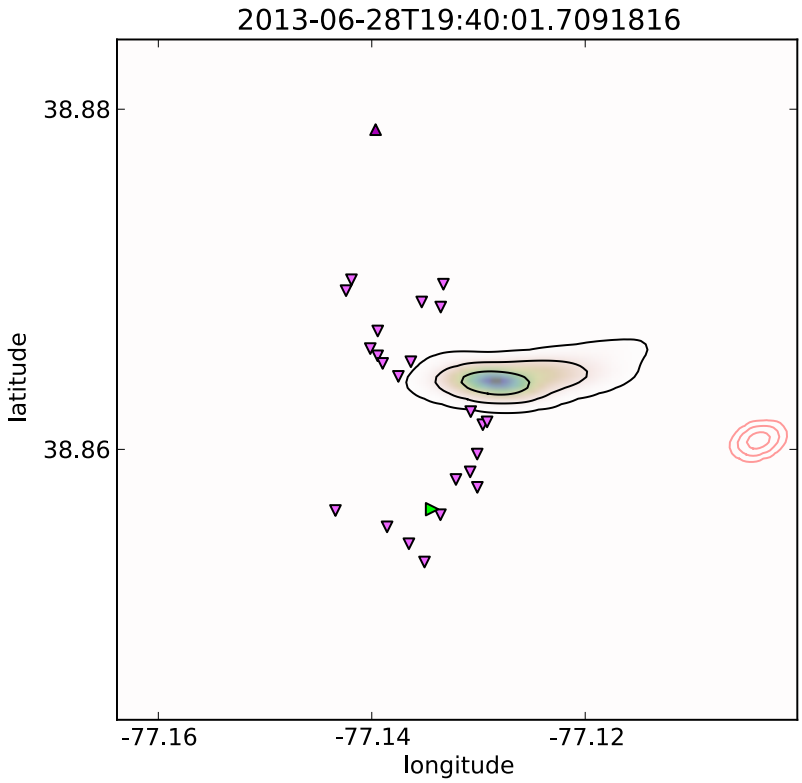

Figure 54: Location of seventeenth pulse. In the middle of previously illuminated channel sections, but far from the VHF within 5 milliseconds. Had we assumed gaussian timing errors, we would have located this pulse in an entirely different location, see red contours.

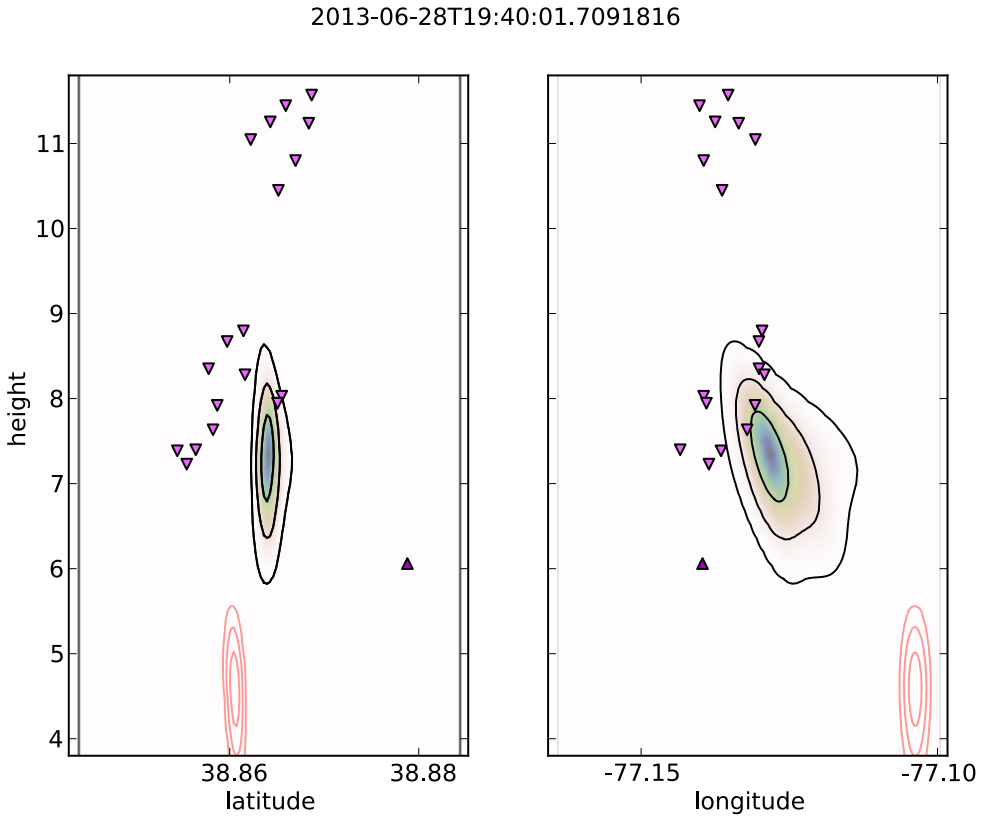

Figure 55: Vertical location of seventeenth pulse. Had we assumed gaussian timing errors, we would have located this pulse in an entirely different location, see red contours.

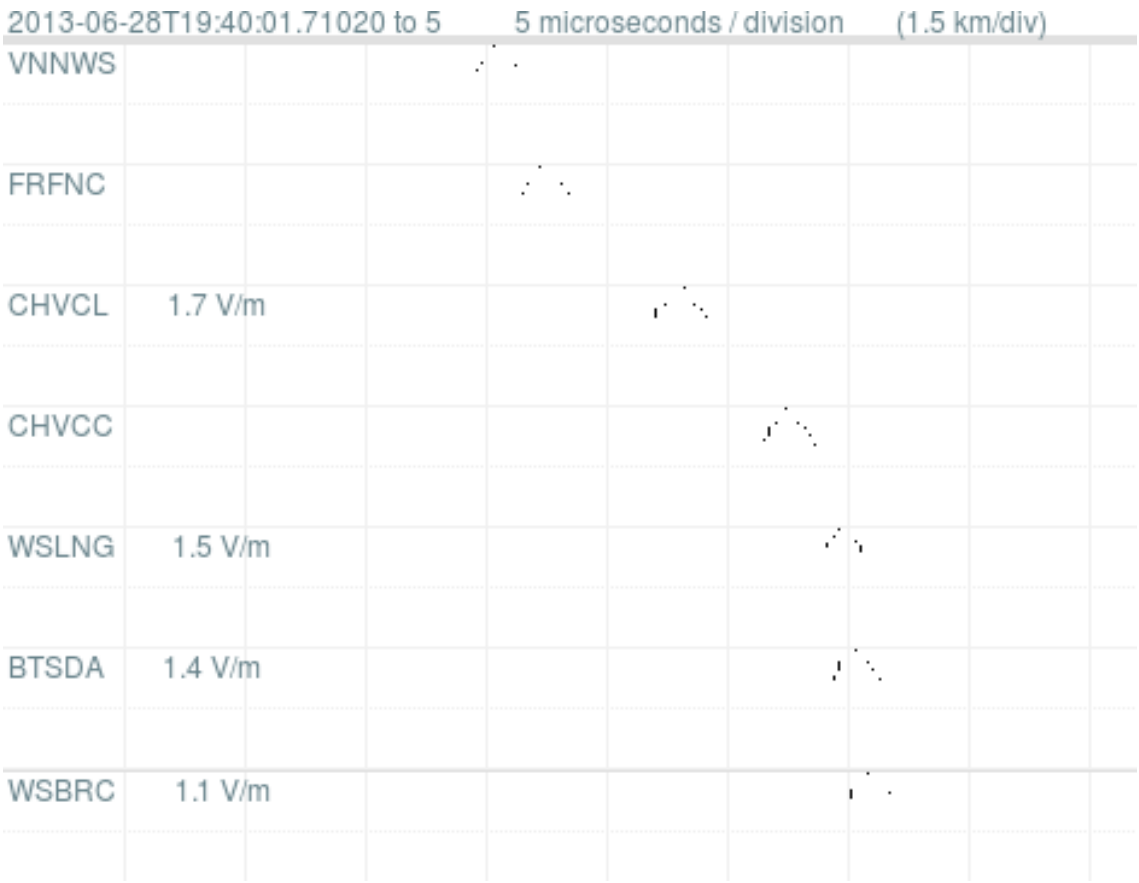

Figure 56: Electric field for eighteenth pulse. Positive radiation field.

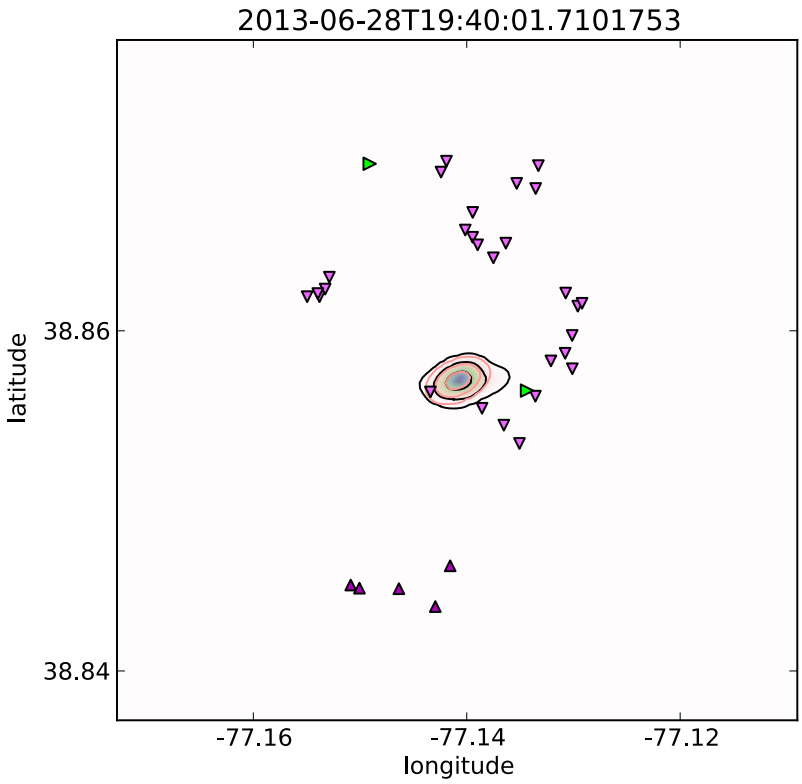

Figure 57: Location of eighteenth pulse. In the middle of previously illuminated channel sections.

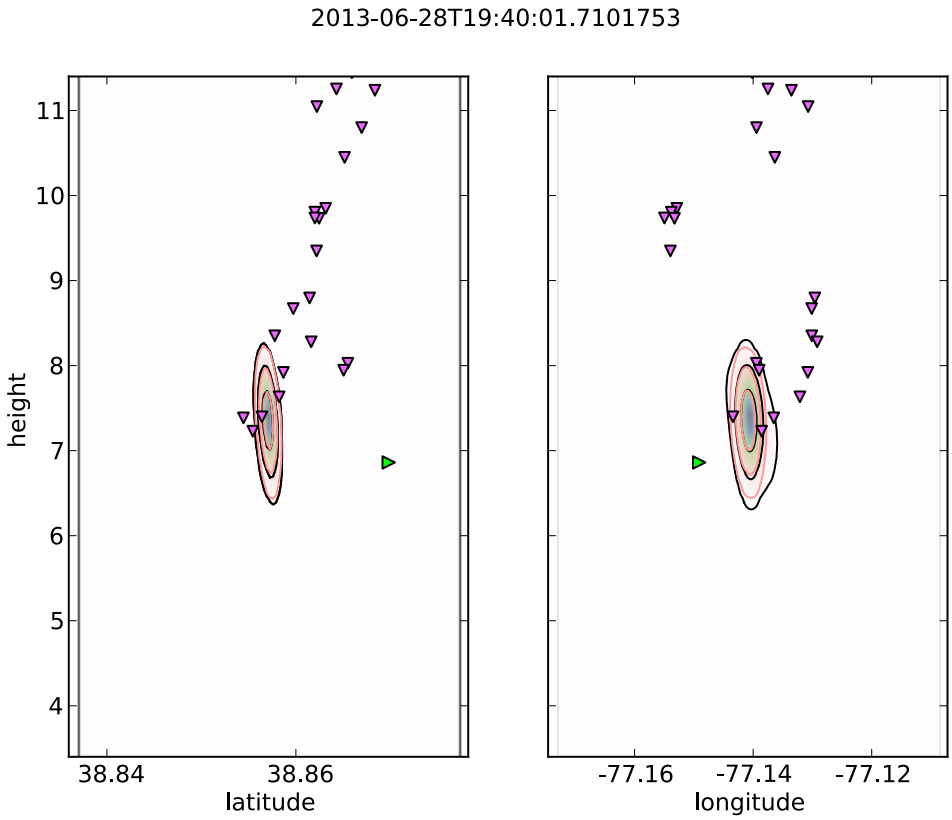

Figure 58: Vertical location of eighteenth pulse. In the latitude versus height plot, it appears that the low frequency pulse is at the lower end of one branch of the channel, and the VHF source is an the lower end of the other branch. Or maybe one or both of these pulses are mislocated.

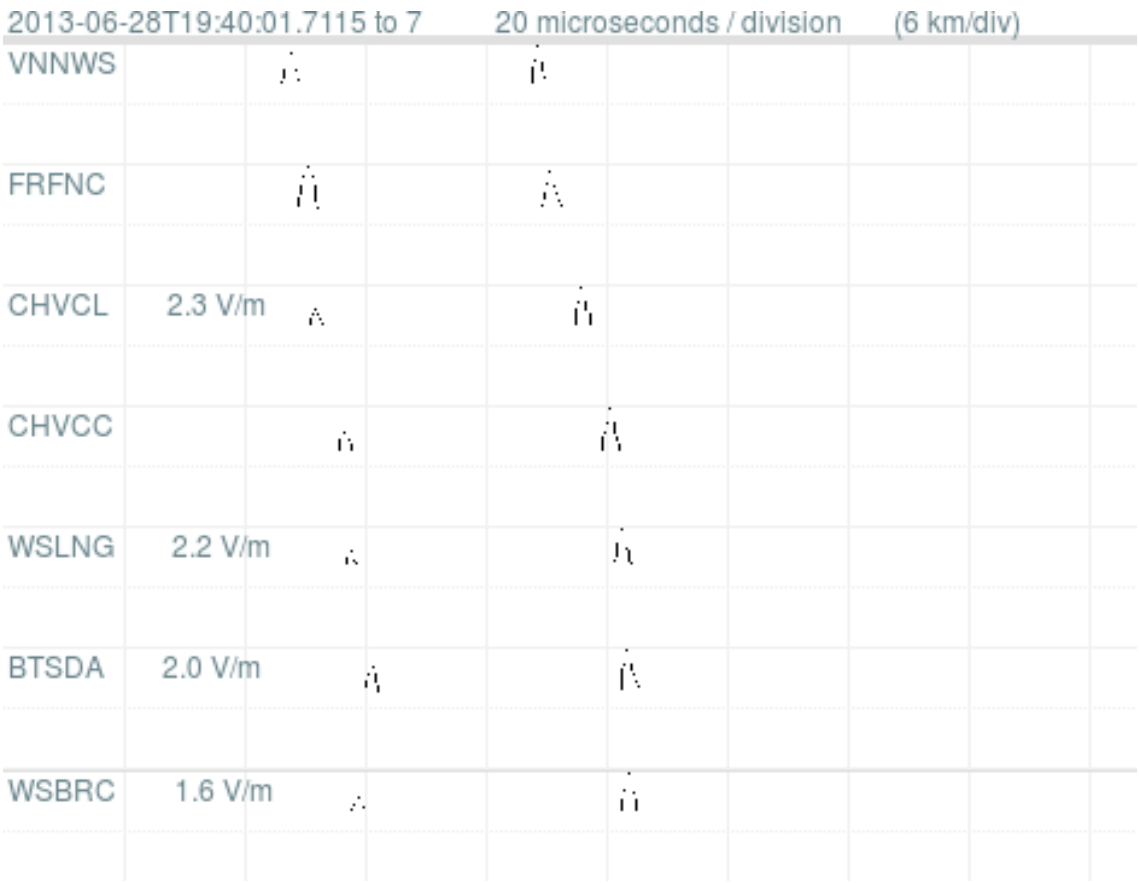

Figure 59: Electric field for nineteenth pulse. Positive pulse pair.

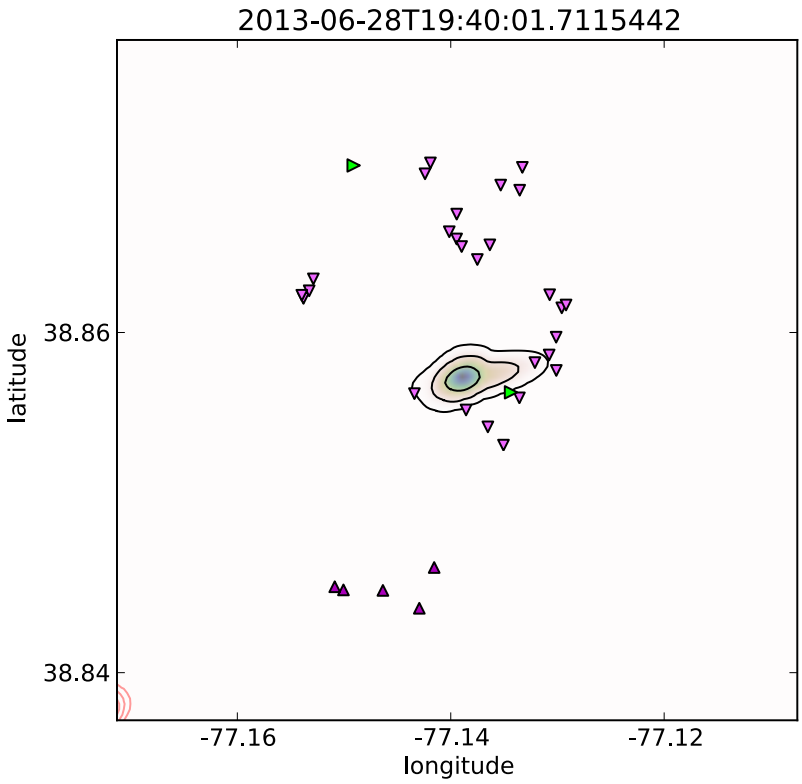

Figure 60: Location of nineteenth pulse. Roughly same location as previous pulse.

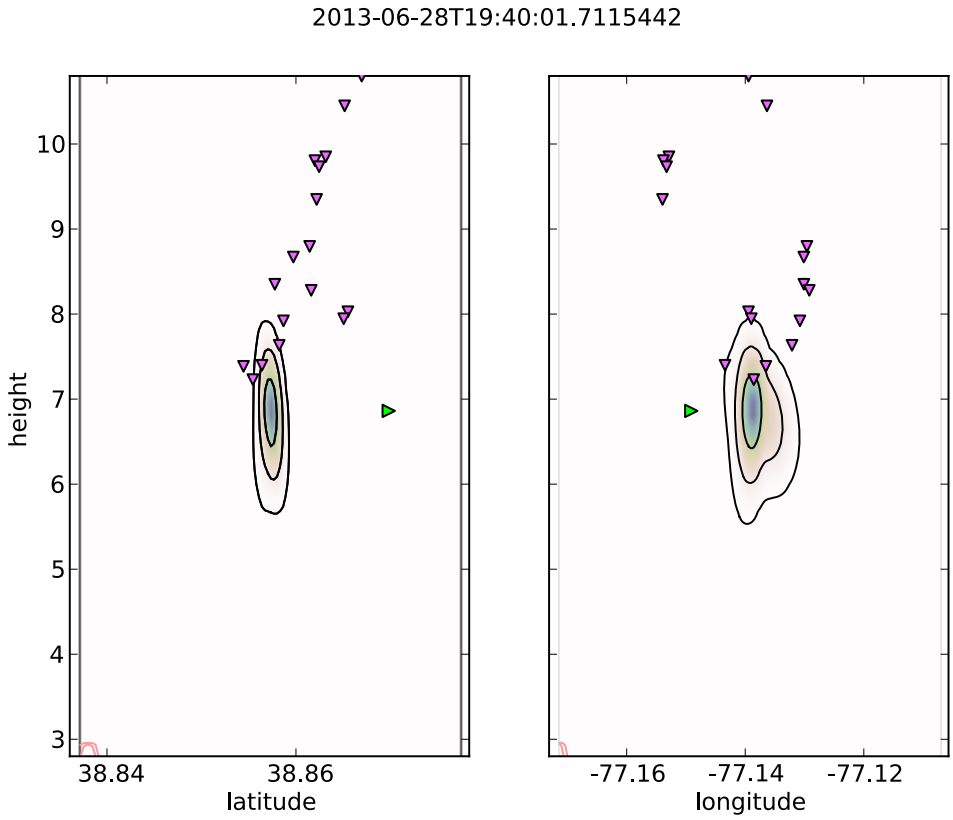

Figure 61: Vertical location of nineteenth pulse. Roughly same location as previous pulse.

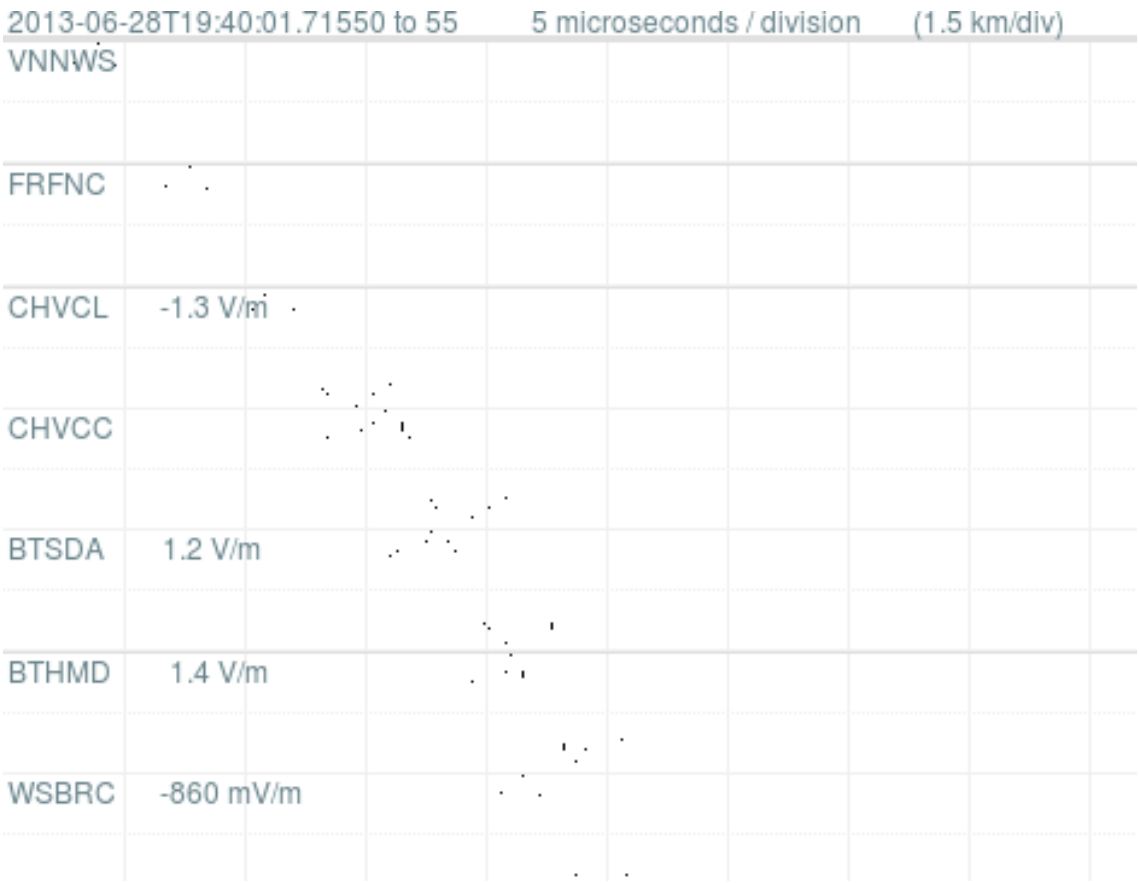

Figure 62: Electric field for twentieth pulse. Positive pulse pair.

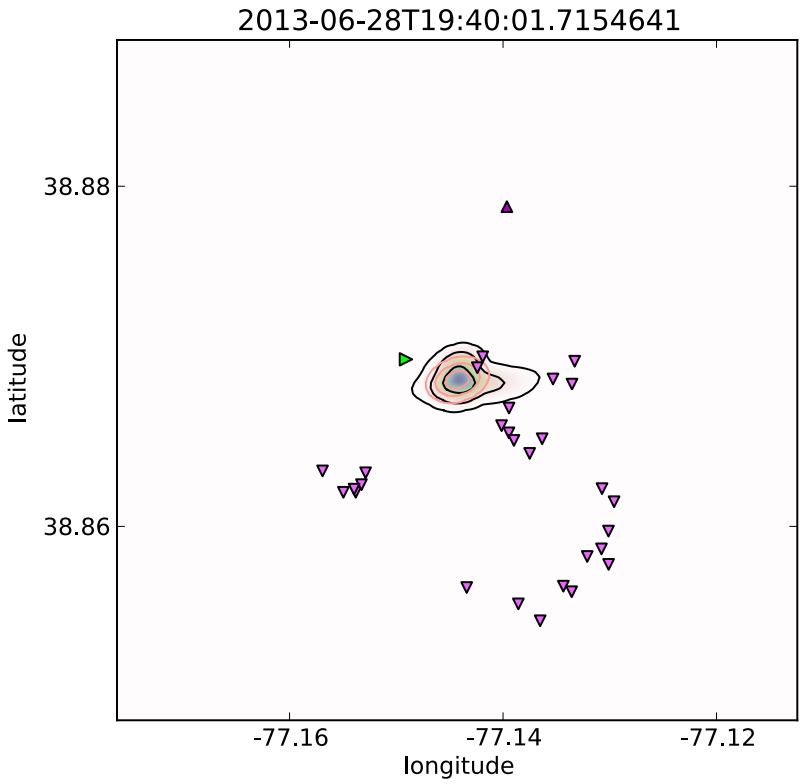

Figure 63: Location of twentieth pulse. Between VHF and old channel.

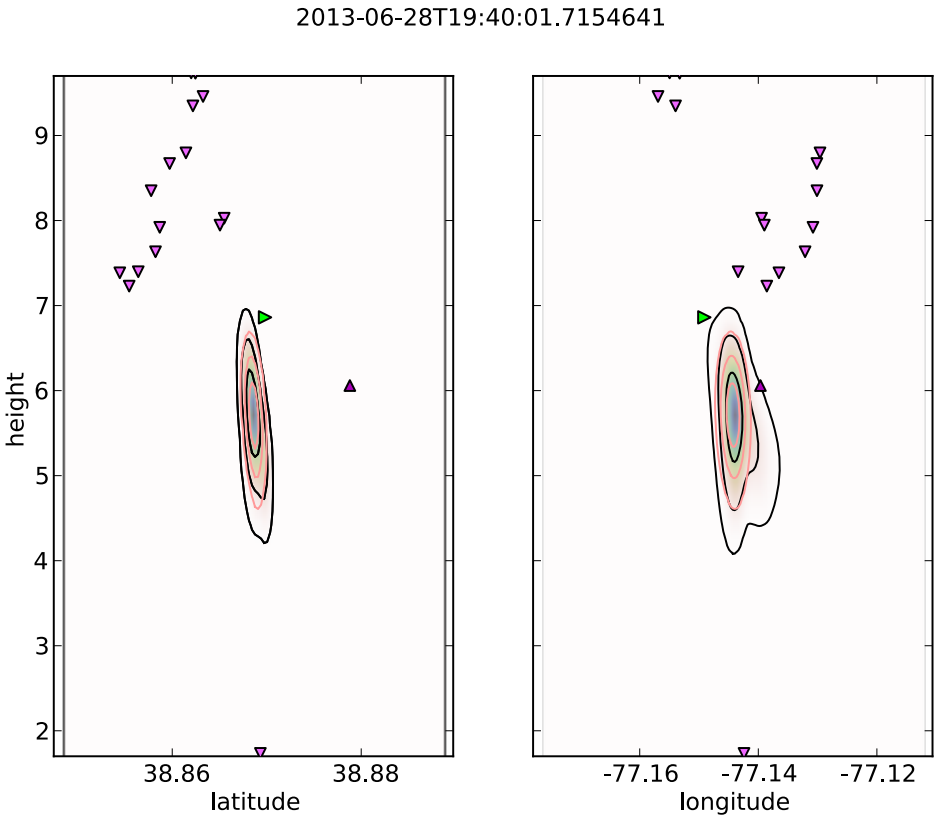

Figure 64: Vertical location of twentieth pulse. Lower than any other pulse we have located in this flash.

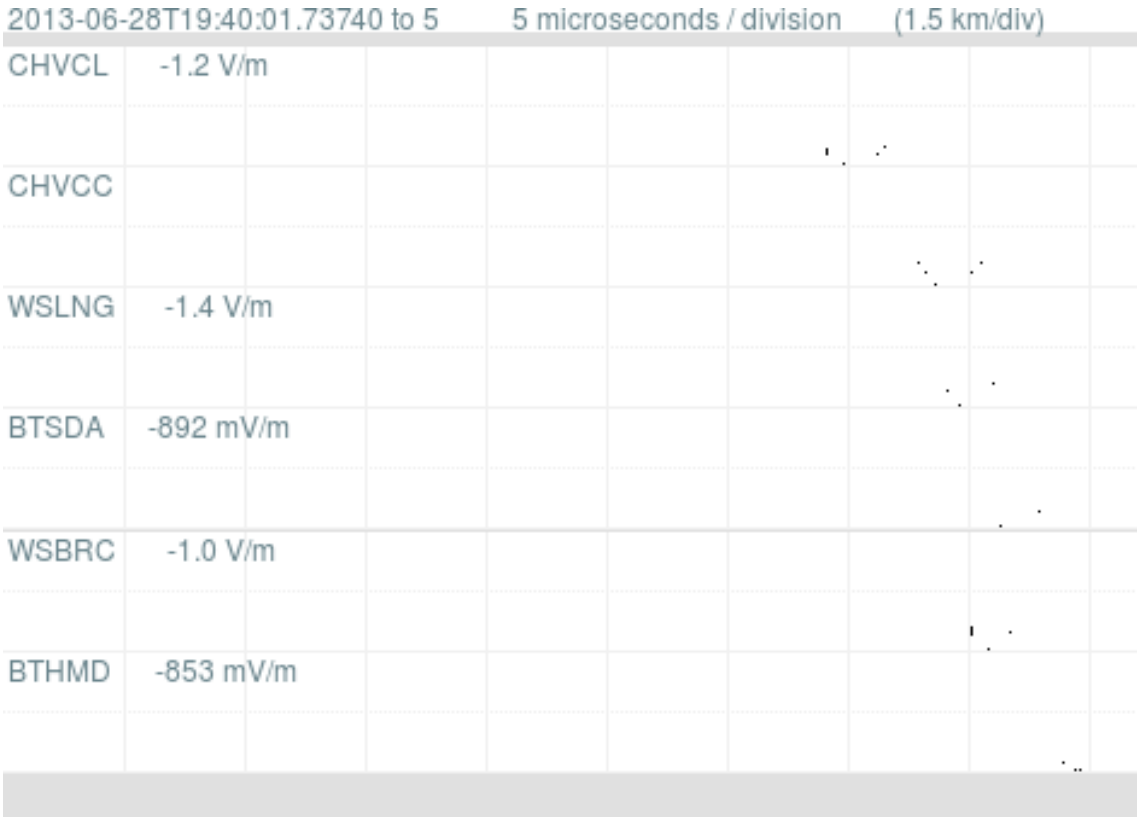

Figure 65: Electric field for twenty first pulse. Fourth negative radiation field pulse of this flash.

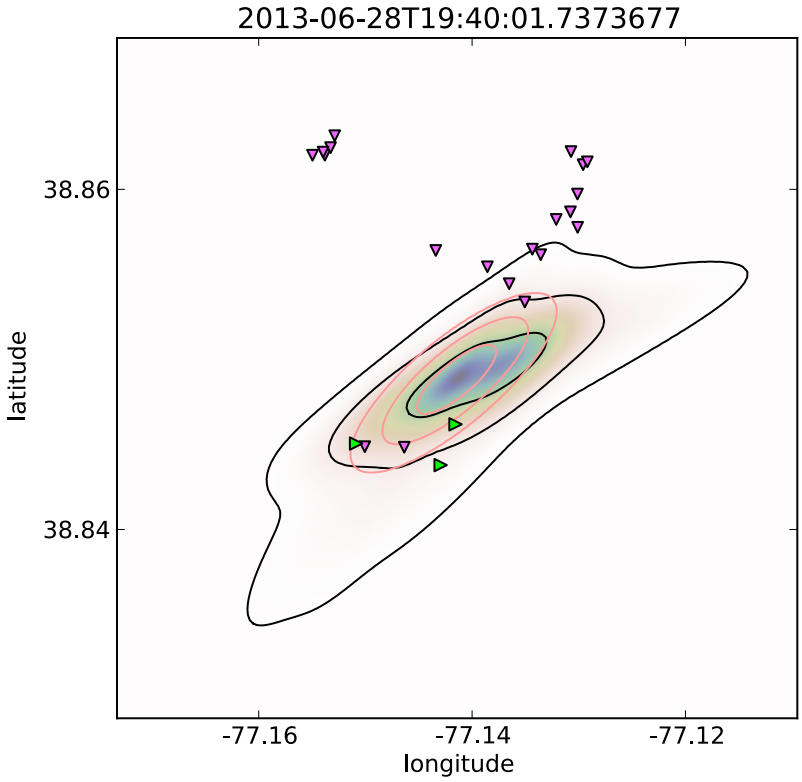

Figure 66: Location of twenty first pulse. Location uncertainty is large.

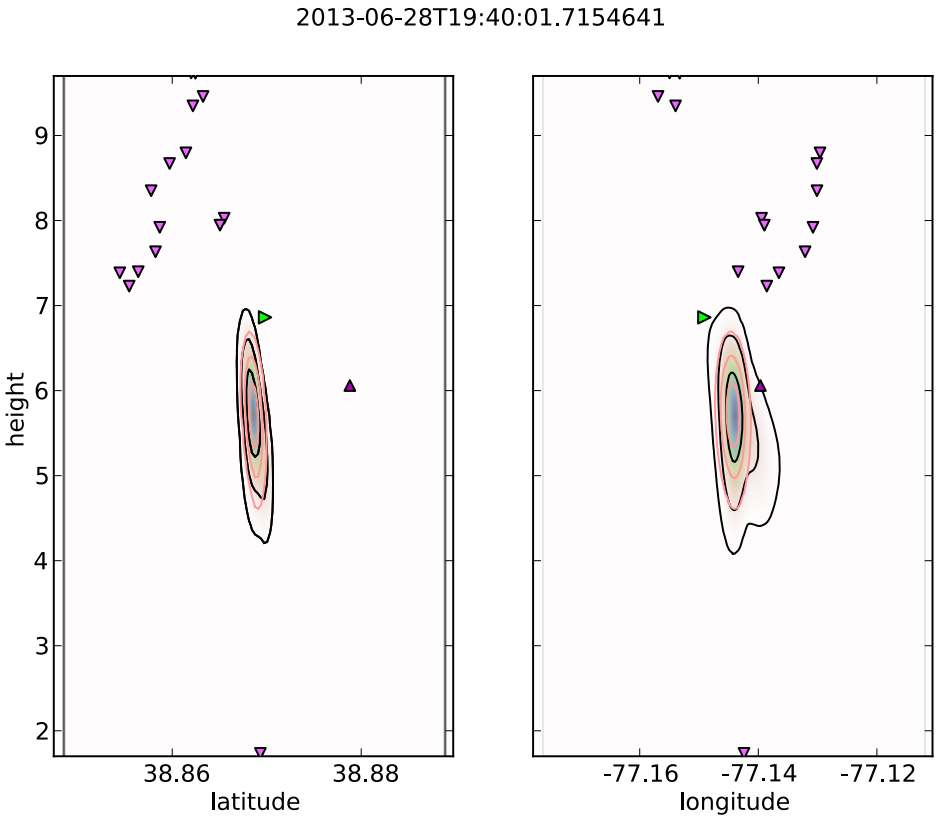

Figure 67: Vertical location of twenty first pulse. Location uncertainty is large.

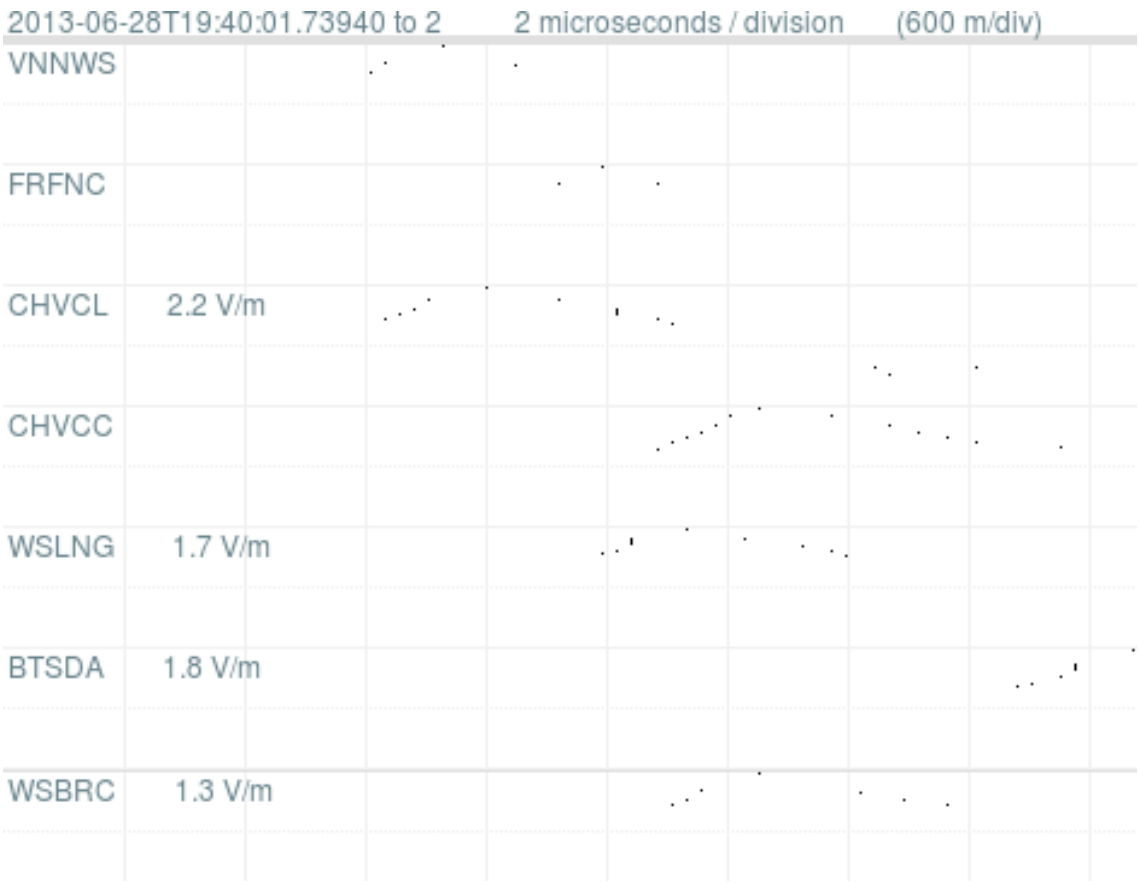

Figure 68: Electric field for twenty second pulse. Lone positive pulse, about 3 microseconds wide.

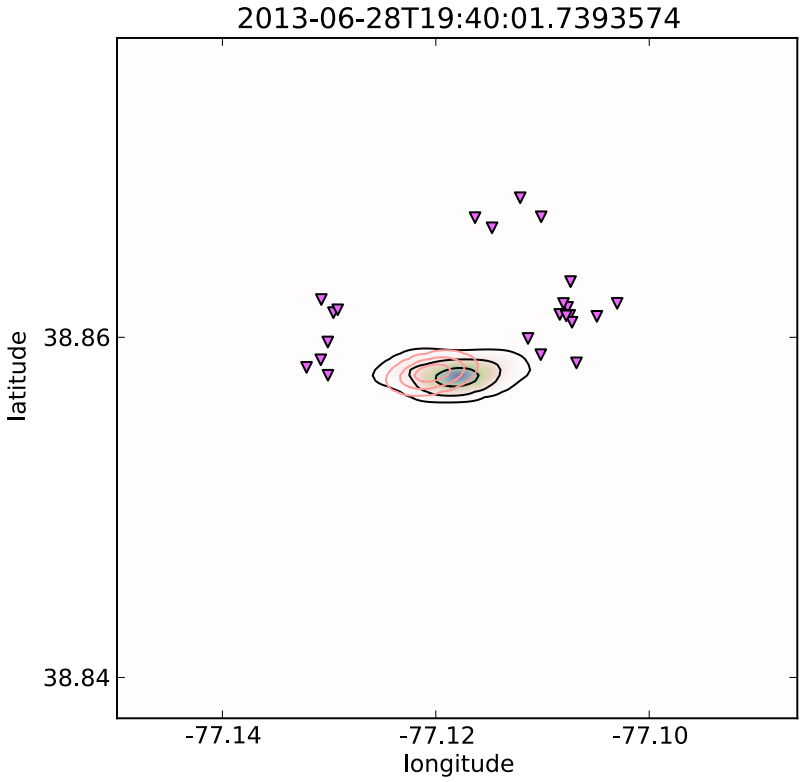

Figure 69: Location of twenty second pulse. Halfway between east and west flash sections.

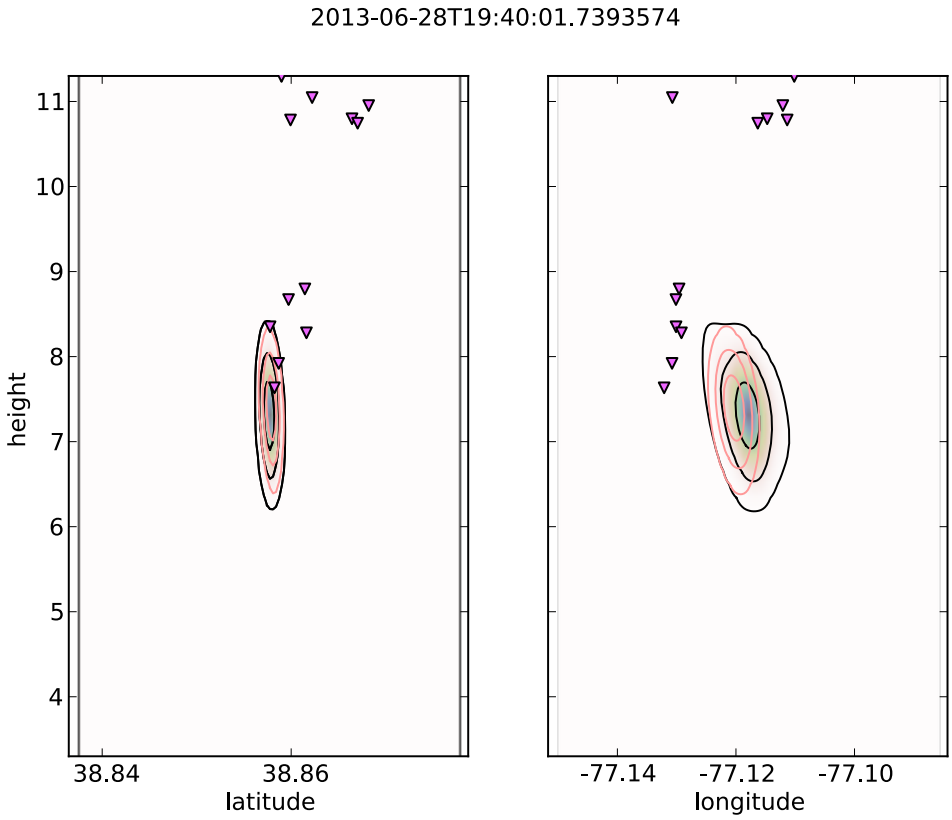

Figure 70: Vertical location of twenty second pulse. Low.

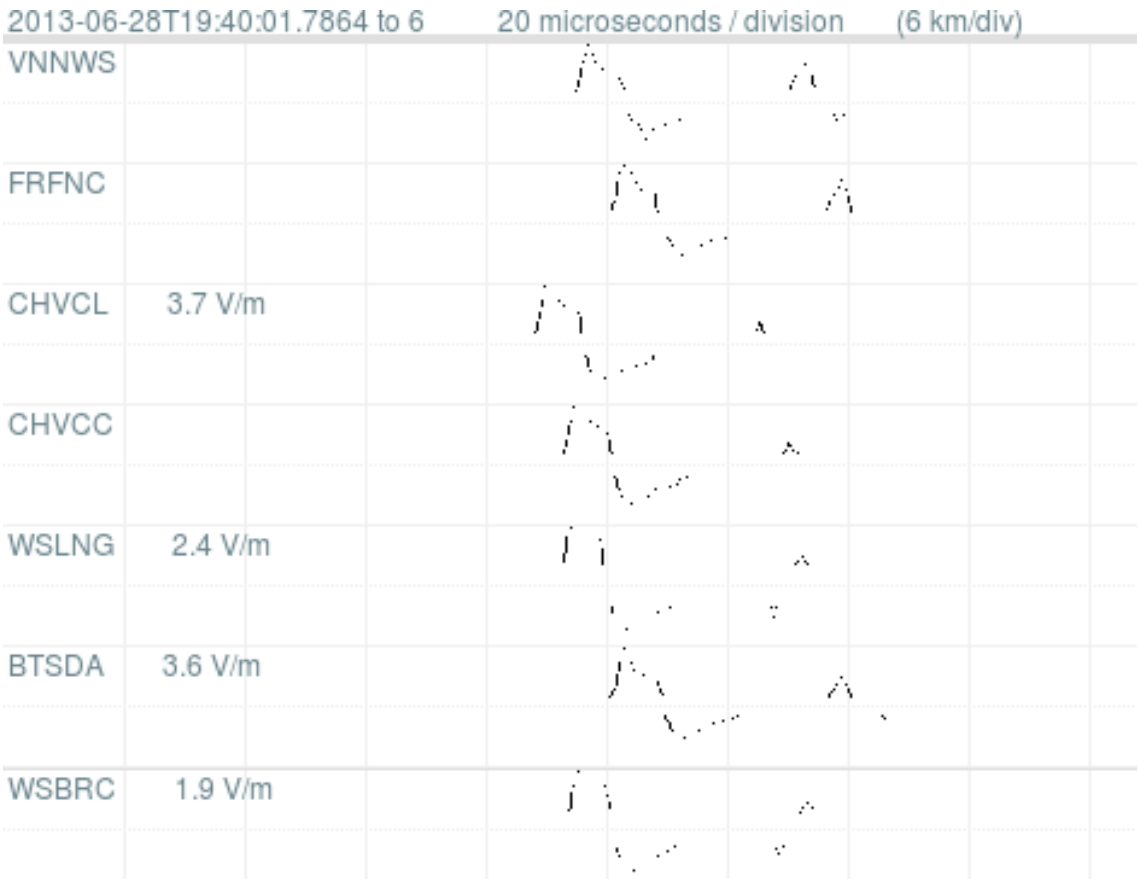

Figure 71: Electric field for twenty third pulse. Long positive pulse, positive part about 8 microseconds wide, followed by long negative overshoot and a second positive pulse. This is a different shape than other pulses in this flash.

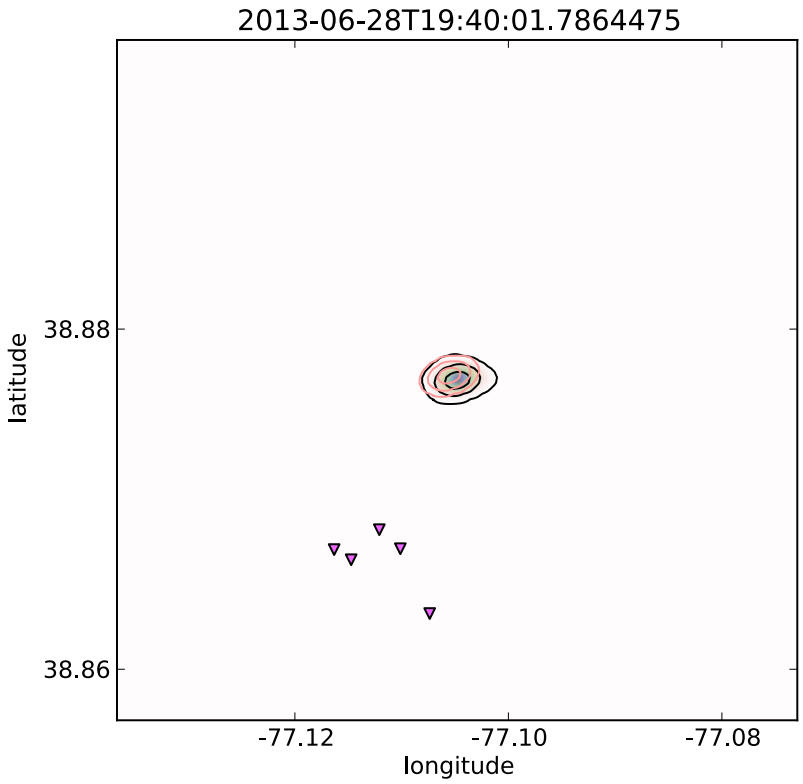

Figure 72: Location of twenty third pulse. Far from VHF.

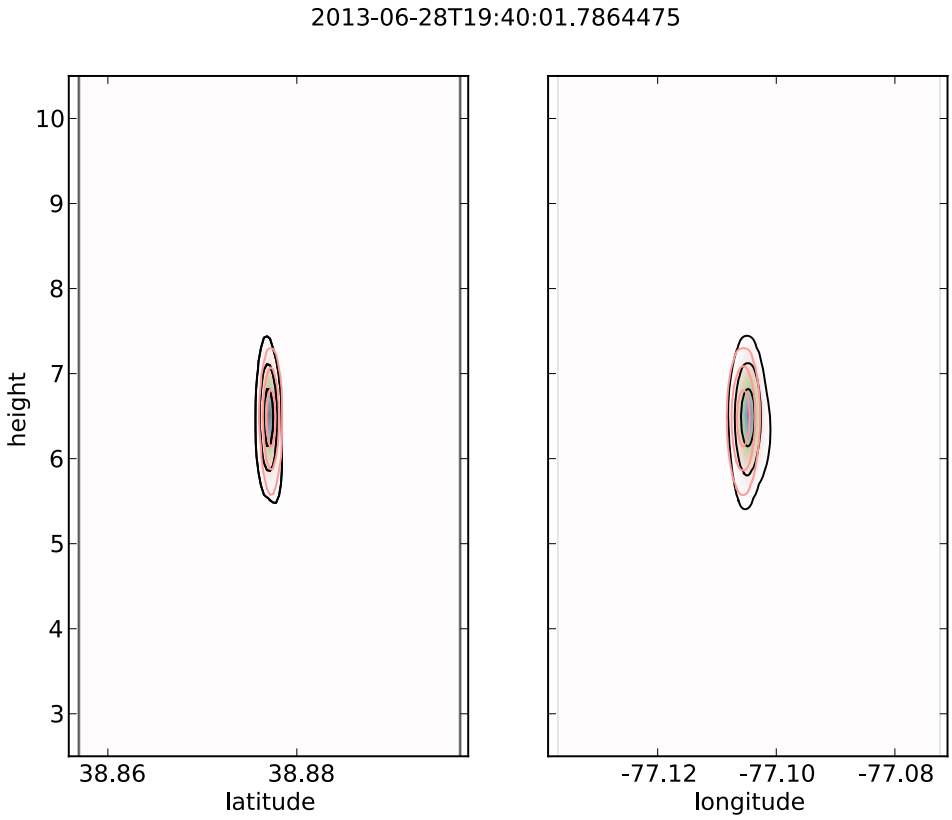

Figure 73: Vertical location of twenty third pulse. Low.

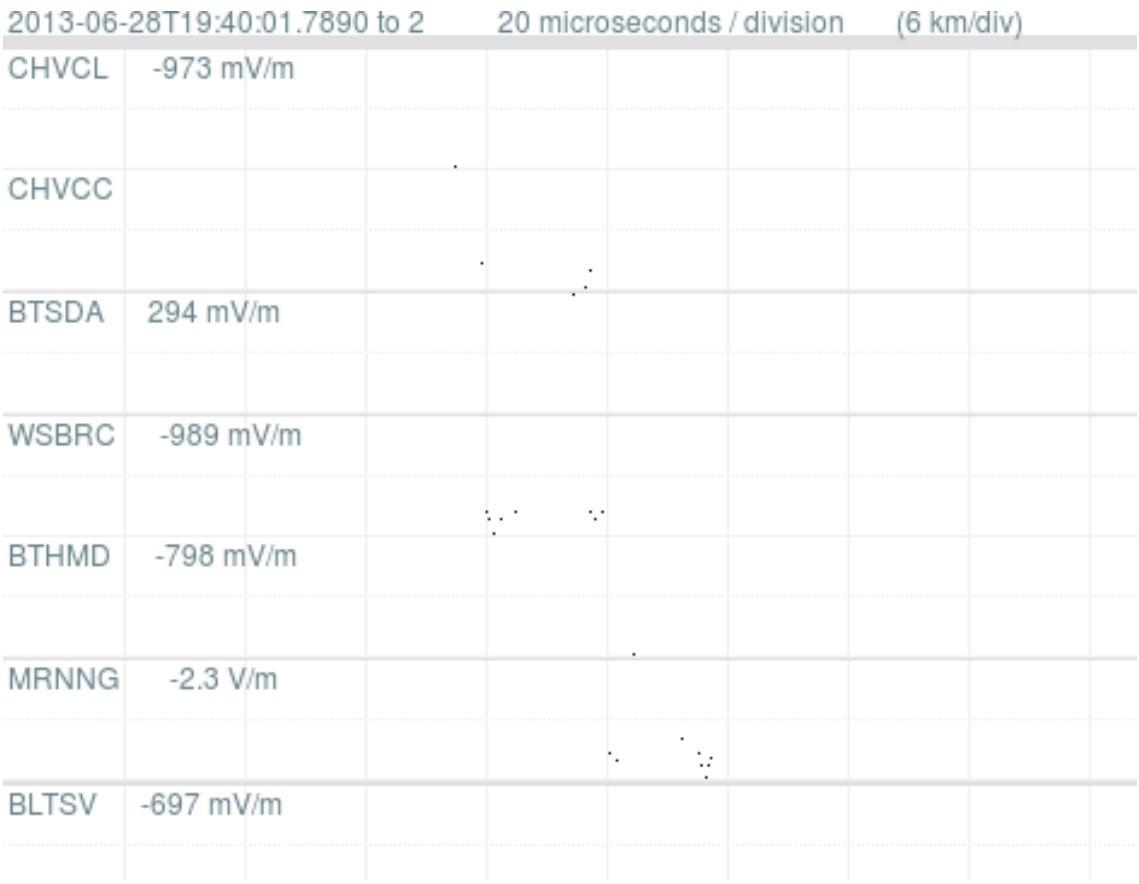

Figure 74: Electric field for twenty fourth pulse. Negative radiation field, barely visible. Unclear whether this is one or two pulses.

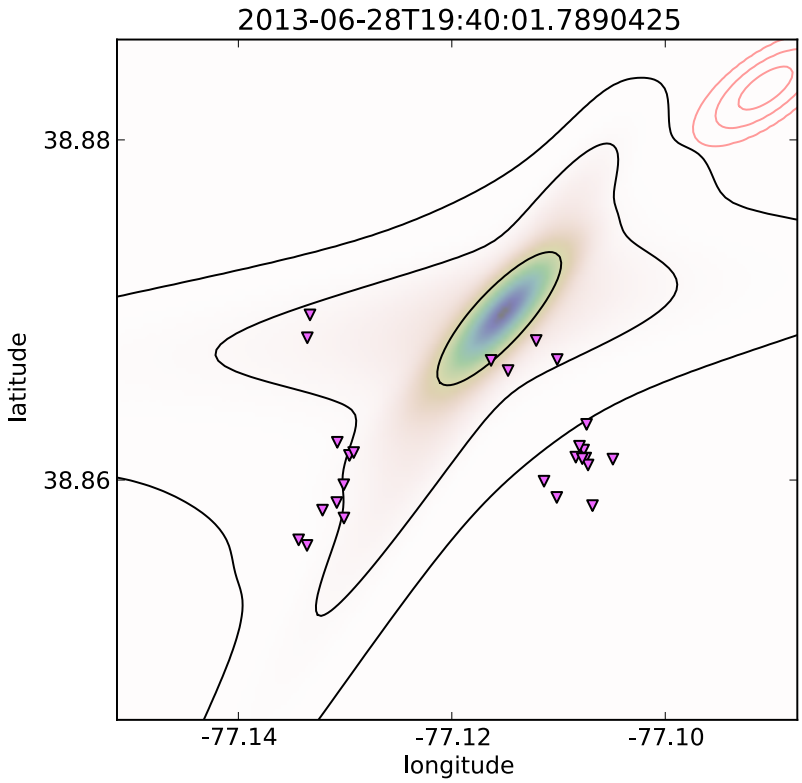

Figure 75: Location of twenty fourth pulse. Location extremely uncertain. Innermost black ellipse contains 50% of the total probability. Middle odd shaped black contour contains 90% of the total probability, and outermost contour, which doesn't quite fit in the plot bounds, contains 99% of the total probability. If we had assumed our timing errors were gaussian (red ellipses), we would have located this flash to the northeast of this point, far from the VHF.

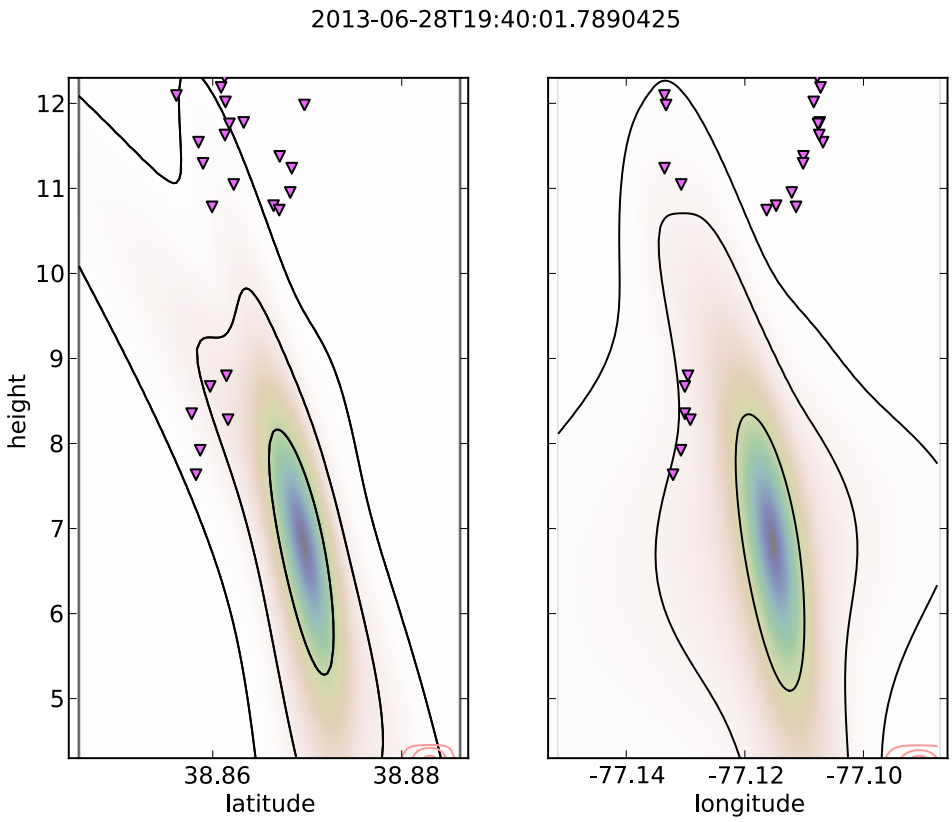

Figure 76: Location of twenty fourth pulse. Location extremely uncertain. Center is below all the VHF, so probably wrong. Innermost black ellipse contains 50% of the total probability. Middle odd shaped black contour which doesn't quite fit in the plot bounds contains 90% of the total probability, and outermost contour, which extends well beyond the plot bounds, contains 99% of the total probability. If we had assumed our timing errors were gaussian (red ellipses), we would have located this flash to the northeast of this point, far from the VHF. Or at least we would have located it there if we used the same sites to compute the solution. Probably we would have detected that this location was bad, and either rejected this pulse entirely, or perhaps tried using different combinations of sites until we found a consistent solution. Given how poor the waveforms for this pulse are, we probably would have rejected it entirely if we were assuming Gaussian timing errors.

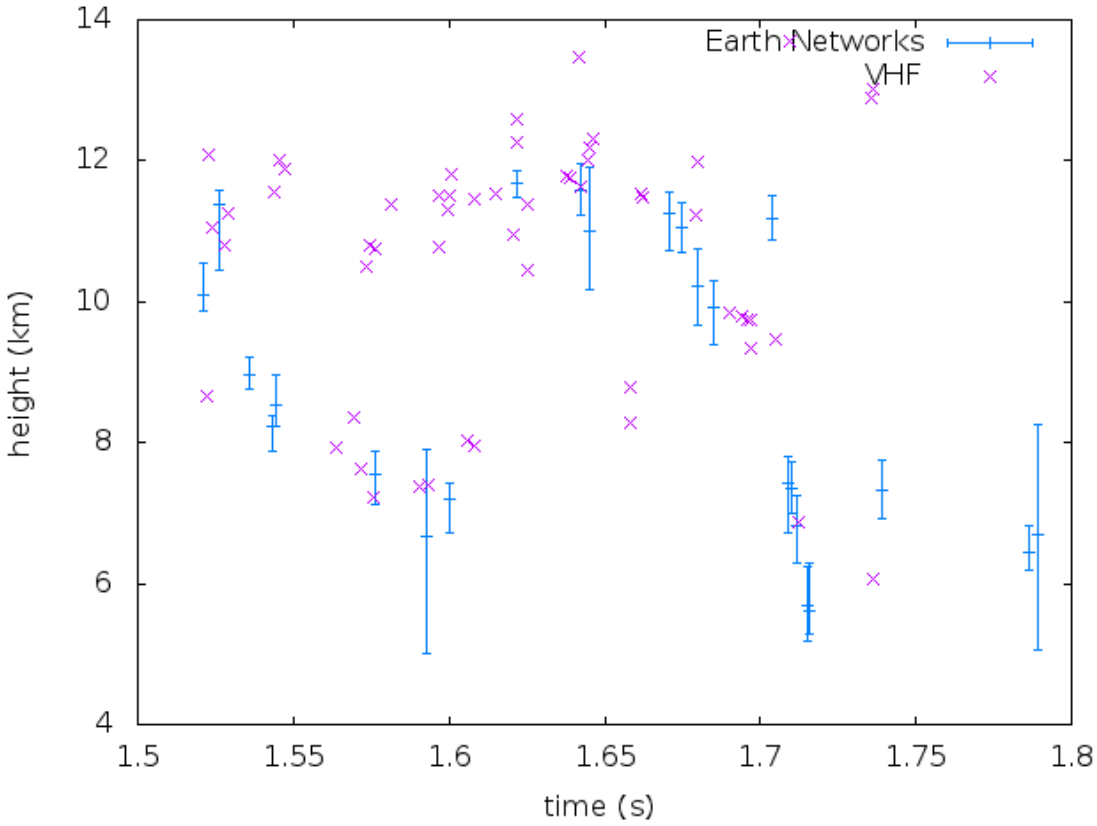

Figure 77: Height of Earth Networks pulses and VHF sources versus time.